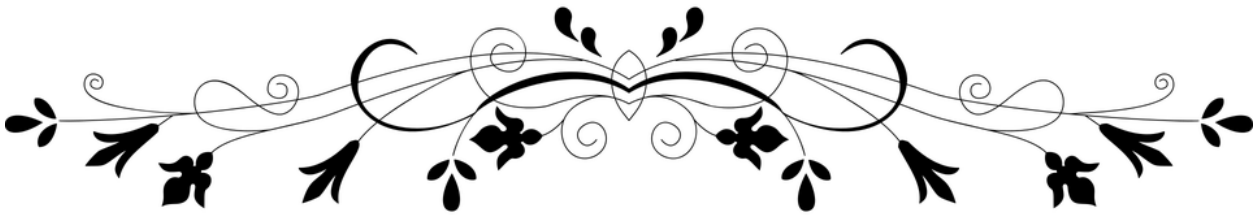

CHAPTER 4

PVA/Chitosan Oligosaccharide Hydrogel

4. Polyvinyl Alcohol/Chitosan Oligosaccharide hydrogel for controlled drug delivery

In the previous chapter, we have discussed hydrogel system made up of polyvinyl alcohol and chitosan lactate (water soluble). While developing these hydrogel systems, we used water as a solvent to dissolve chitosan lactate. It may be due to its chemical structure and larger polymeric chain. The biocompatibility of chitosan lactate is limited. Therefore, another chitosan derivative, chitosan oligosaccharide was studied to develop a hydrogel system along with polyvinyl alcohol which will be introduced in this chapter. Chitosan oligosaccharide is known to be soluble in water at room temperature, owing to its small polymeric chains.

Hydrogel composites from PVA and Chitosan have been developed by various researchers as a function of their composition for various medical applications. The application of chitosan is limited due to its solubility in acidic solvent only. This shortcoming can be improved by using water soluble chitosan. In this work, PVA-chitosan oligosaccharide (water soluble) is used as a precursor to develop cross linked hydrogel network using a chemical crosslinker. The developed hydrogel is characterized for its swelling behaviour, wettability and microstructure. To know the detail information about the thermal degradation of the hydrogel, kinetic analysis was also performed through mathematical modeling. Additionally, its viscoelastic behaviour was investigated via estimation of stress relaxation profile using Weichert model [78]. Besides, Lomefloxacin loaded hydrogels also suppressed growth of E. Coli bacteria, revealing release of drug in active form.

4.1 Introduction

Hydrogel has attracted significant attention in the area of pharmaceutics[162-167] such as drug delivery[168], wound healing[169], and artificial implants as scaffold[170]. Due to its high water retention capacity and softness, it shows biocompatibility with tissue, displays remarkable resemblance with extracellular matrix[171]. Physically cross-linked hydrogels forms temporary junctions such as hydrogen bonds, ionic or hydrophobic interactions among the polymer chains that provide a reversible three dimensional network. On the contrary, chemical cross-linking leads to formation of permanent junctions facilitated by coalition, hydrogen bonding and crystallization and give a durable and irreversible cross-linked network. The crosslinking was carried out by glutaraldehyde, one of the most commonly used chemical cross-linker for various bioprosthetic implants fabrication[172].

Polyvinyl alcohol, a synthetic polymer, exhibits some unique properties such as biocompatibility, water solubility, chemical resistant and film forming properties, makes it an ideal candidate for the various bioengineering applications. In spite of these desirable properties PVA shows some drawbacks such as high swelling capacity and solubility in aqueous medium. Due to these drawbacks, the mechanical property (Young's modulus) of polyvinyl alcohol based nanocomposite polymeric membrane is very weak[173].

Chitosan, is a natural cationic polymer obtained from deacetylation of chitin. It is the second most abundant polymer found in the nature. Chitosan oligosaccharide is produced from Chitosan through enzymatic and chemical method. Its molecular weight (3900 Da) is very less than Chitosan. It is water soluble, non-toxic, anti-inflammatory and antioxidant[174]. Jiliang Wu et al. developed Chitosan polycaprolactone based scaffold, loaded with microsphere, containing transforming growth factor for articular

cartilage repair[175]. André R. Fajardo et al. synthesized chitosan/chondroitin sulfate films containing silver sulfadiazine in their matrix for wound healing applications [176]. EmeseBiró et al. prepared chitosan particle and its efficiency for the immobilization of β-galactosidase was evaluated [177], where, Atta Rasool et al synthesized Chitosan poly (N-vinyl-2-pyrrolidone) based hydrogel as a wound dressing material [178]. VaishaliPawar et al. reported that, drug can be conjugated with hydrogel matrix of chitosan and its potential, as a sustained drug delivery matrix [179].

Similarly, several different research works has been reported based on chitosan based formulations for different biomedical applications. But these formulations were developed by dissolving chitosan in dilute acids [180-186]. Due to dissolution of chitosan in acidic environment, its application to clinical use is limited. To avoid acid soluble chitosan use, aqueous soluble chitosan is needed.

Motivated by this rationale, we developed composite hydrogel based on polyvinyl alcohol and chitosan oligosaccharide (water soluble) using glutaraldehyde as a crosslinker and its biocompatibility evaluation was performed. Till date very few works has been reported as polyvinyl alcohol Chitosan oligosaccharide based hydrogel for Lomefloxacin delivery system. Lomefloxacin hydrochloride is considered a potent antibiotic against Gram positive and Gram negative bacteria. It is used for various medical applications such as for the treatment of bronchitis and urinary tract infections. This antibiotic has been explored less concerning other antibiotics [131, 187-189].The developed hydrogel system was characterized by XRD, FTIR, DSC TGA, SEM and AFM. Mathematical modeling was used to acquire mechanical parameters and thermal kinetics parameters.

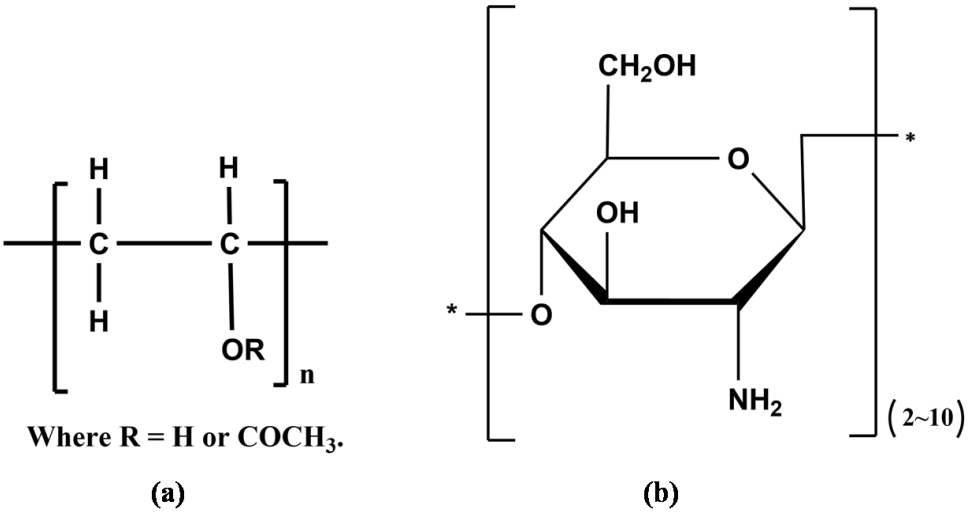

Figure 4.1-Structure of (a) PVA and (b) Chitosan oligosaccharide**.**

4.2 Materials

Polyvinyl alcohol (Molecular Weight 1,15,000, Hydrolysis 99%), and chitosan oligosaccharide (CO) were purchased from Loba Chemie and Sisco Research Laboratories, India respectively. Glutaraldehyde solutions ((25% w/w) and Hydrochloric acid was purchased from Loba Chemie, India. Glutaraldehyde reagent was prepared by mixing 5 mL of glutaraldehyde (25% w/w) in 10 mL of ethyl alcohol and Hydrochloric acid as catalyst.

4.3 Synthesis of Hydrogel

Polyvinyl alcohol- Chitosan oligosaccharide composite hydrogels were developed by chemically crosslinking through glutaraldehyde (Figure 4.1). Briefly, 10% w/v PVA in distilled water solution was prepared by autoclaving at 121^{o}Cfor 1 hour. Then, chitosan oligosaccharidesolution of five different concentrations 0.25%, 0.5%, 1%, and 2% w/v were prepared by dissolving required amount of chitosan oligosaccharide in distilled water. 10 mL of 10% w/v PVA solution, 3.5 mL of chitosan oligosaccharide solution of

each concentration and 10 mL of water were mixed using magnetic stirrer. Then glutaraldehyde reagent (0.5 mL) as cross linker was added to the above solution with continuous stirring. Now, 20 mL of resultant solution was casted into polystyrene petridish (Tarson, Internal diameter 8.5 cm) and kept in incubator at temperature 37^{o}Cfor 48 hours. After drying, films were peeled off from the petridish. Five different hydrogels samples were made with different ratios of each constituent as shown in the table 1. All the hydrogel samples were washed with water, followed by soaking them into 0.1 M glycine solution for 1 hour [131].These samples were dried in vacuum oven and stored properly.

Table 4.1: Composition of Polyvinyl alcohol chitosan oligosaccharide hydrogel composite

Sample Code	10 % PVA Solution (mL)	Water (mL)	Chitosan Oligosaccharide(CO) Solution		Crosslinker (mL)
			Concentration (% W/V)	Quantity (mL)	
PCO-1	10	10	0	3.5	0.5
PCO-2	10	10	0.25	3.5	0.5
PCO-3	10	10	0.5	3.5	0.5
PCO-4	10	10	1	3.5	0.5
PCO-5	10	10	2	3.5	0.5

4.4 Characterizations

4.4.1 X ray diffraction analysis

To know the crystalline behavior of raw materials and developed hydrogels, X ray diffraction (Rigaku Miniflex 600 desktop X ray diffraction System, Japan) study was performed. This diffractometer possess CuKα as a radiation source filtered through graphite monochromator (wavelength=0.15 nm). In this instrument, x ray is generated at 40 KV and 15 mA. X ray diffraction pattern was obtained at 2 theta scan range of 10

- 60 degree, scan speed (duration time) of 5 degree/ minute and step width of 0.0200 degree. To quantify crystallinity, degree of crystallinity was calculated using following formula[190]

$$Degree\ of\ Crystallinity = \frac{crystalline\ area}{Crystalline\ area + Amorphous\ area}$$

4.4.2 Thermal analysis

Differential Scanning Calorimetry (NETZSCH DSC 204 F1 PHOENIX) of all the hydrogel samples was performed in the range of 50^{o}Cto 250^{o}Cin inert atmosphere.In thermogravimetric analysis, change in weight of sample was measured as function of change in temperature. Thermogravimetric analysis (Perkin Elmer-STA 6000) of hydrogel samples were performed in the range of 50 ^{o}C to 600 ^{o}C.

4.4.3 Fourier transform infrared spectroscopy analysis

In order to know, functional group of hydrogel composites, Fourier transform infrared spectroscopy (Perkin Elmer IR spectrophotometer with deuterium as IR source (USA) in the range of 400 to 4000 cm^{-1}, with resolution of 4 cm^{-1}. To obtain FTIR spectra of powder samples, KBr pellet pellets were used, whereas for hydrogel sheets ATR mode was used. All FTIR spectra were obtained through 8 scans.

4.4.4 Stress relaxation analysis

In order to know the mechanical behavior of hydrogels, stress relaxation test of hydrogels was performed (TA-HD-Plus, Stable Micro Systems, Haskmere, England). The rectangular shaped hydrogel sample of size 60 mm × 5 mm was clamped into the machine. During this study, effective sample length of 50 mm was used. To perform this test, stretching rate was set to 1 mm/ sec till 5 mm distance. To get stress relaxation pattern, sample was fixed at this condition for 1 minute.

4.4.5 Surface morphology analysis

Surface morphology was studied using scanning electron microscopy (FEI QUANTA 450**)** analysis. The atomic force microscopy (NTEGRA Prima, Germany) was performed to study the surface topology of the hydrogel.

4.4.6 Contact angle analysis

Contact angle study of all the hydrogels were performed to know the wettability of the developed hydrogel composites. Contact angle of all the developed hydrogels were measured using Kruss F-100 tensiometer. It has basically two major components, sample holder and solvent holder. In this study, we have used water as test fluid to measure the contact angle of hydrogel samples. At the top of tensiometer, sample holder is placed, whereas solvent holder was placed at the bottom of tensiometer. Contact angle study was performed by adopting Whilhelmy plate method. To measure contact angle, dimension (length× width× thickness) of each sample was measured and fed into the associated software of tensiometer. Then sample was allowed to move towards solvent (test fluid). As sample comes in contact with interface of water, contact angle value was displayed on computer. Similarly, Contact angle measurement was performed for all the hydrogel samples.

4.4.7 Swelling behavior analysis

To know the water holding capacity of the hydrogel, swelling of the hydrogel was performed using phosphate buffer (pH 7.4) at 37^{o}C. The weight variations of swollen hydrogels were measured as function of time. The swelling index of hydrogels were computed using following formula, 4.1-

$$\%\, Swelling\ Index\ = \frac{\mathrm{Wt-Wo}}{\mathrm{Wo}} \times 100 \qquad (4.1)$$

where W_o and W_t is the initial weight of hydrogel and weight after time t respectively.

4.4.8 Drug loading and release analysis

To load drug into the hydrogels, swelling equilibrium approach was adopted[134]. Briefly, hydrogel sample size 1 cm × 1 cm was subjected to swell in Lomefloxacin hydrochloride solution (20 mL, 0.2% w/ v) for 24 hour. In order to know the drug release pattern from hydrogels, these drug loaded hydrogel sheets, were placed into dialysis membrane (Molecular weight cut off 12kDa) and dipped into beaker having phosphate buffer saline (PBS) solution as drug releasing medium (pH 7.4) at temperature 37^{o}C. This beaker was placed into incubator to achieve continuous shaking and small volume (4 mL) of drug releasing medium was withdrawn at different time period followed by its absorbance measurement using UV VIS Spectrophotometer at 280 nm. The released drug concentration at different time period was computed using calibration curve. Further to know, the release mechanism the drug released data was fitted into Korsmeyer Peppas equation[191].

$$F= k*(t)^{n} \quad (4.2)$$

where F represents fraction of drug release over time t. K and n represents constant and release exponent respectively.

4.4.9 Drug loading efficiency evaluation

Drug loading efficiency of developed hydrogels was calculated according to reported literature with some modification[192]. During this process, drug loading medium was kept at constant temperature and specific pH. Hydrogel sample of dimension 1cm^2 was kept into 30 mL Lomefloxacin drug solution containing 21 mg of Lomefloxacin drug for 24 hours. After attaining equilibrium, hydrogel sample were blotted using filter paper and weight of each hydrogels were measured followed by drug loading efficiency calculations.

4.4.10 Antimicrobial evaluation

Antimicrobial activity of composite hydrogels were estimated by Disc diffusion method, according to reported work with some modifications[125]. To perform this test E. coli bacteria was used. Briefly, nutrient agar was prepared and sterilized for half an hour at 15 pounds (lbs) per square inch pressure, followed by transfer it into petridish (Tarson). Then 100 µl E.coli suspension was inoculated to solidified agar. Then control, blank hydrogel, and drug loaded hydrogel samples were placed over these petridish followed by incubation for 48 hours at 37^{o}C. To prepare control sample, disc shaped filter paper was saturated with Lomefloxacin Hydrochloride drug (concentration 1 mg/mL). After 48 hours, zone of inhibition formed was measured.

4.4.11 In vitro cell viability and cell imaging

The cells were cultured in Dulbecco's modified Eagle' medium and maintained at 37 ^{o}Cand 5% CO_2. The washed hydrogel films were sterilized using 70% alcohol. Then these films were excised into square sheet of 3×3 mm^2 and placed into tissue culture plate. To perform this study, 96 well tissue culture plate were used. Each well of these tissue culture plate were occupied with 200 µL media and cell density of 1× 10^4 cells per well. The wells without hydrogel samples were considered as control. To remove dead cells, the cultured cells were washed after 24 hour with 1 mM PBS. These tissue culture plates were placed in incubator for 24, 48 and 72 h respectively. To estimate cell viability at 24 hour and cell proliferation at day 2 and day 3, MTT assay of all the samples were performed. MTT assay is used to measure the activity quotient of live cell. MTT assay involves conversion of 3-(4, 5-dimethylthiazol-2-yl)-2,5–diphenyltetrazolium bromide (MTT) into formazen by living cell. After incubation, the culture media and hydrogel sheet were removed from the well of tissue culture plate.100 µL of MTT (0.5 mg/mL MTT) solution was further added and then incubated

for 4 hour at 37 ºC. To dissolve formazen, 100 µL of DMSO was added in each well of culture plate followed by absorbance measured at 570 nm using a microplate ELISA plate reader. In order to understand, the death of cell upon treatment with hydrogel, fluorescent microscopy was performed. L 929 cell line, having density of 1×10^4 cells per mL was suspended in fresh medium and seeded into 24 well plates and incubated for 24 hour. After that, old media was replaced by fresh media and again incubated for 24 hour. Then, washing of cells was performed using PBS, followed by staining with fluorescent dye acridine orange and ethidium bromide at a concentration of 100 µg/ mL each. After staining, the cells were incubated at room temperature for next half an hour. In order to acquire image of cells, fluorescence microscope (Dewinter Technologies, India) was used.

4.5 Results and Discussion

4.5.1X ray diffraction analysis

X ray diffraction study of all the raw materials and hydrogel samples was performed and shown in the figure 4.2. XRD spectrum of PVA shows two diffraction peaks, one sharp peak at 2θ angle of 20º and other small, broader peak at 41º. The peak at 20º can be attributed to the PVA crystallite[193]. Whereas, chitosan oligosaccharide displayed a broad peak at 25º showing its amorphous nature. From XRD spectra of PVA and chitosan oligosaccharide, it can be stated that PVA exhibits more crystallinity than chitosan oligosaccharide. Crystalline materials exhibits many sharp peaks and amorphous materials such as glass and liquids shows broad peak in their XRD spectra[194]. The composite hydrogels prepared from polyvinyl alcohol and chitosan oligosaccharide shows peak at 20º. The percentage crystallinity of PCO-1, PCO-2, PCO-3, PCO-3, PCO-4, PCO-5 was found to be 75.2%, 73.7%, 79.6%, 76.40% and

70.3% respectively. Based on the calculated crystallinity of hydrogel composite, we can conclude that except PCO-3 and PCO-4, crystallinity of hydrogel composite reduces with addition of chitosan oligosaccharide. Similar type of loss in crystallinity result was obtained by Mahato et al during the synthesis of Polyvinyl alcohol and chitosan lactate based hydrogel composite [6].

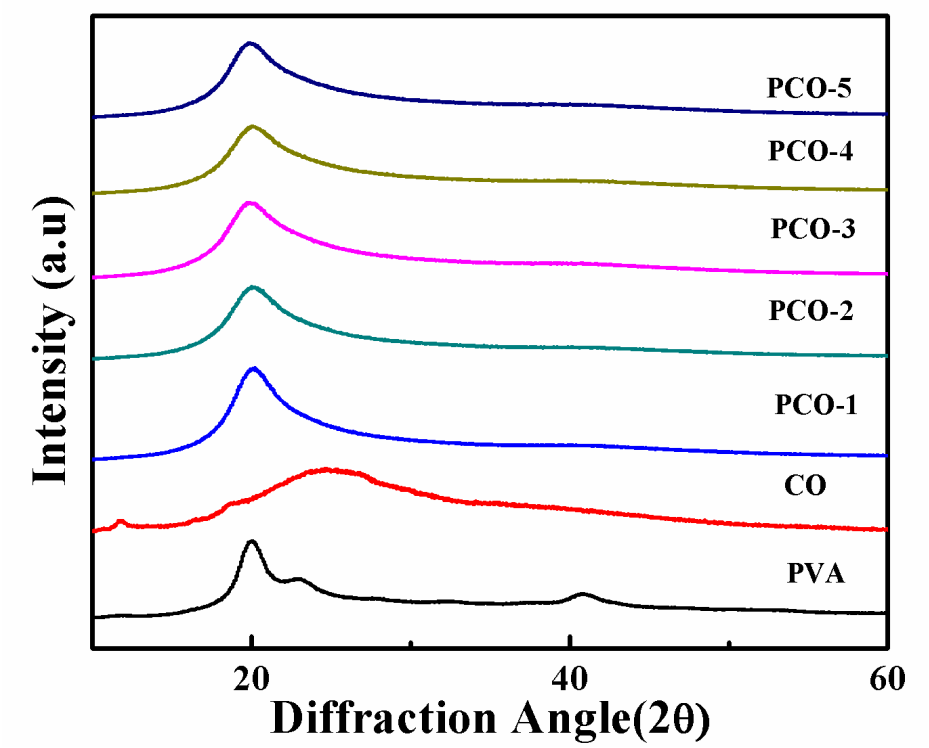

Figure 4.2: XRD Study PVA powder, Chitosan Oligosaccharide powder and hydrogel Composites.

4.5.2Thermal analysis

The DSC result (figure 4.3) of developed hydrogels depicts that first endothermic peak of PCO-1 hydrogel was found at 33 ^{o}C, whereas second endothermic peak was found at 105^{o}C. PCO-3 hydrogel showed first endothermic peak at 30^{o}C and second endothermic peak around 103^{o}C. PCO-5 hydrogel displayed first endothermic peak around 31^{o}Cand second endothermic peak at 105^{o}C. The slight variation in first endothermic peak was observed due to addition of chitosan oligosaccharide, resulting into restricted polymer

chain movement in the composite hydrogel. Similar type of result was obtained by Seira Morimune in polyvinyl alcohol/ graphene oxide nanocomposite[195]. It is important to note that, third endothermic peak of PCO-5 hydrogel was shifted to lower temperature with respect to PCO-1 and PCO-3 hydrogel. It occurs due to the suppression of crystallinity in PCO-5 hydrogel. This result was also supported by XRD spectra of composite hydrogels. The obtained DSC data of the hydrogels depicts that the position of endothermic peak of all the hydrogels are different. It may be due to different water holding capacities of different hydrogels. Besides, the difference in the position of endothermic peak can be due to the difference in hydrogel composite water interaction. Similar type of result was obtained by C.G.T. Neto et al with Chitosan poly(ethylene oxide)(PEO) composite[196]. From the TGA graph (figure 4.4), it is clear that developed hydrogels were showing weight loss in three stages. PCO-1 hydrogel showed slow weight loss till 119 ^{o}C. This loss occurs due to the removal of moisture from the sample. PCO-1hydrogel showed higher weight loss between 119^{o}C to 416^{o}C. It occurs due to the decomposition of polymeric network of the hydrogel. Third stage weight loss in PCO-1 hydrogel was observed between 416^{o}C to 467^{o}C. It occurs may be due to degradation of hydrogel. Similarly, PCO-3 showed weight loss in three stages, stage 1 weight loss between 0^{0}C to 119^{0}C, stage 2 weight loss between 119 ^{o}C to 420 ^{o}C and stage 3 weight loss between 420^{o}C to 475^{o}C. PCO-5 showed initial weight loss between 0 ^{o}C to 119 ^{o}C and second stage weight loss occurs between 240 ^{o}C to 425^{o}C and third stage loss occurs between 425 ^{o}C to 465 ^{o}C. From, the TGA graph, it is clear that all the composite hydrogels exhibits weight loss in three stages. Among these hydrogels, PCO-5 hydrogel shows slightly more stable behavior. This is may be due to formation of more compact hydrogel network. The compact network results due to rise in their concentration in composite hydrogel. The enhancement in the thermal stability of PCO-

5 is due to glutaraldehyde mediated cross linking between PVA and chitosan oligosaccharide. Increase in the amount of chitosan oligosaccharide concentration in the composite hydrogels promotes the formation of Schiff base due to the chemical association of PVA and chitosan oligosaccharide[196].

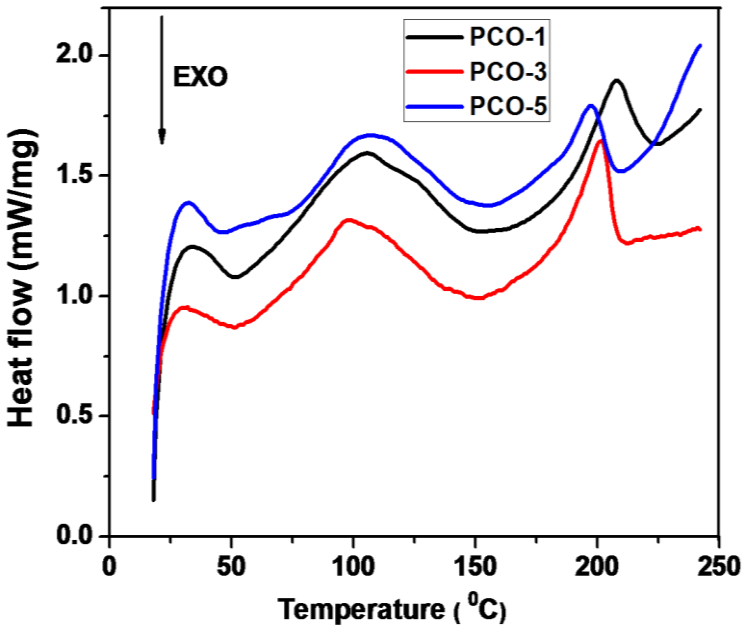

Figure 4.3: DSC study of PCO Composite Hydrogels.

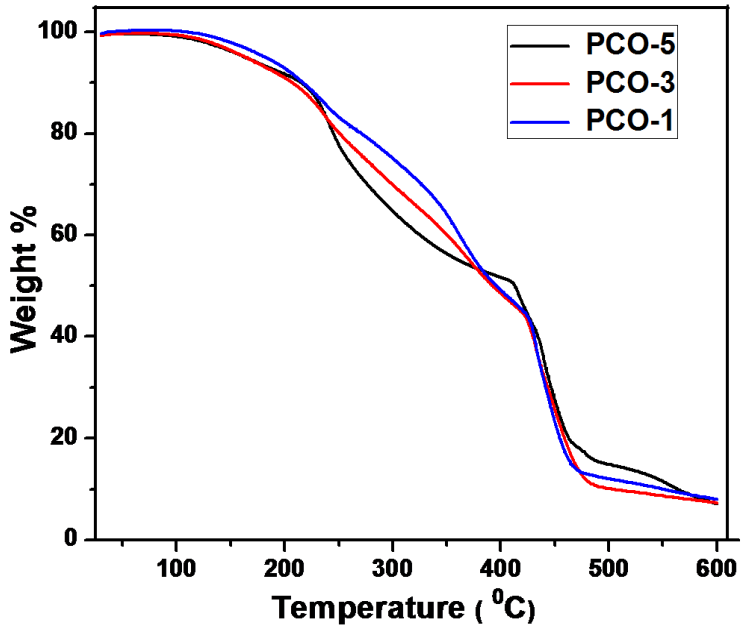

Figure 4.4: TGA study of PCO Composite Hydrogels.

To get in-depth analysis of thermal degradation, kinetic parameters of hydrogel system was obtained by performing mathematical modeling using TGA data. TGA was performed in nitrogen atmosphere and kinetic reaction parameters were obtained from Arrhenius equation as shown in equation 4.3 [197].

$$k = Ae^{-E/RT} \tag{4.3}$$

where k, A, R, T, E represents rate constant, frequency factor, universal gas constant, absolute temperature, and activation energy of the reaction.

Global kinetics of the reaction can be written as-

$$\frac{-1}{wo-wf}\frac{dw}{dt} = k * \left(\frac{w-wf}{wo-wf}\right)^n \tag{4.4}$$

where w_o, w_f, w, dw/dt and n represents initial mass at the start of thermal degradation, final mass at the end of thermal degradation, mass after time t, ratio of change in mass with respect to time and order of reaction, respectively.

Upon integrating equation (4.3) and equation (4.4), we get following equation-

$$\ln\left[\frac{-1}{W_O-W_f}\frac{dw}{dt}\right] = \ln(A) - \left(\frac{E}{RT}\right) + n\ \ln\ \left(\frac{w-w_f}{w_o-w_f}\right) \tag{4.5}$$

Equation 4.5 can be represented as following equation

$$y = B + Cx + Dz \tag{4.6}$$

where

$$y = \ln\left[\frac{-1}{W_O - W_f}\frac{dw}{dt}\right];$$

$$X = \frac{1}{T}$$

$$Z = \ln\left(\frac{w - w_f}{w_o - w_f}\right);$$

$$B = n(A)$$

$$C = -\frac{E}{R}; \qquad (4.7)$$

$$D = n$$

To determine the value of constants B, C and D, multiple linear regression analysis was performed by MATLAB software in the entire temperature range of hydrogel degradation[198]. Thus, E, A and n value for the current hydrogel (PCO-3) was found to be 18.48 kJ/mol, 1.748 min^{-1} and 0.77 respectively.

We have added curve pertaining to upper and lower values of Confidence Intervals and compared with the fitted curve to show accuracy of the measurement with 95% confidence, as shown in the curve below.

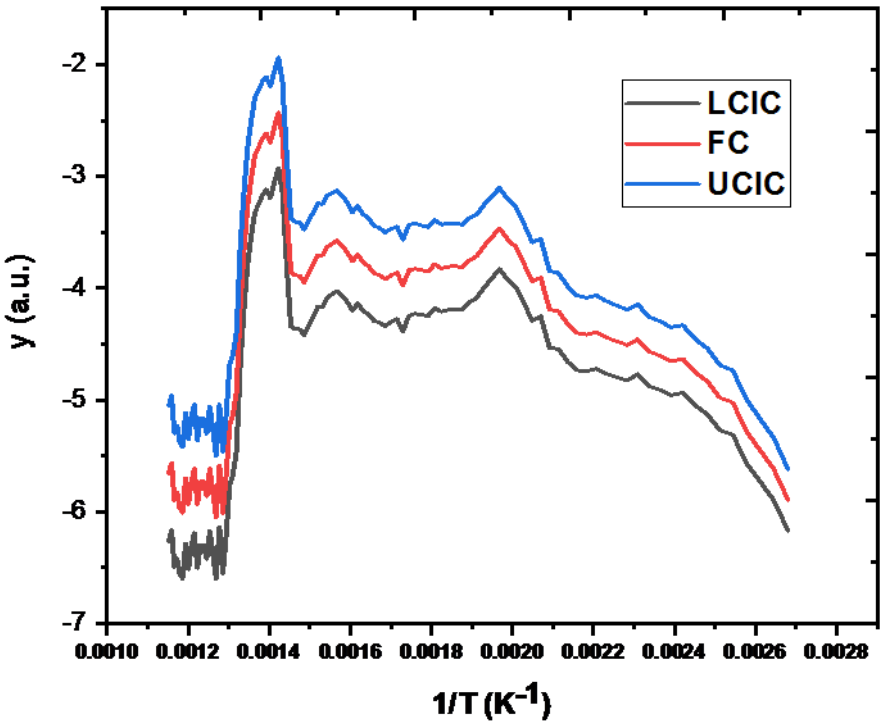

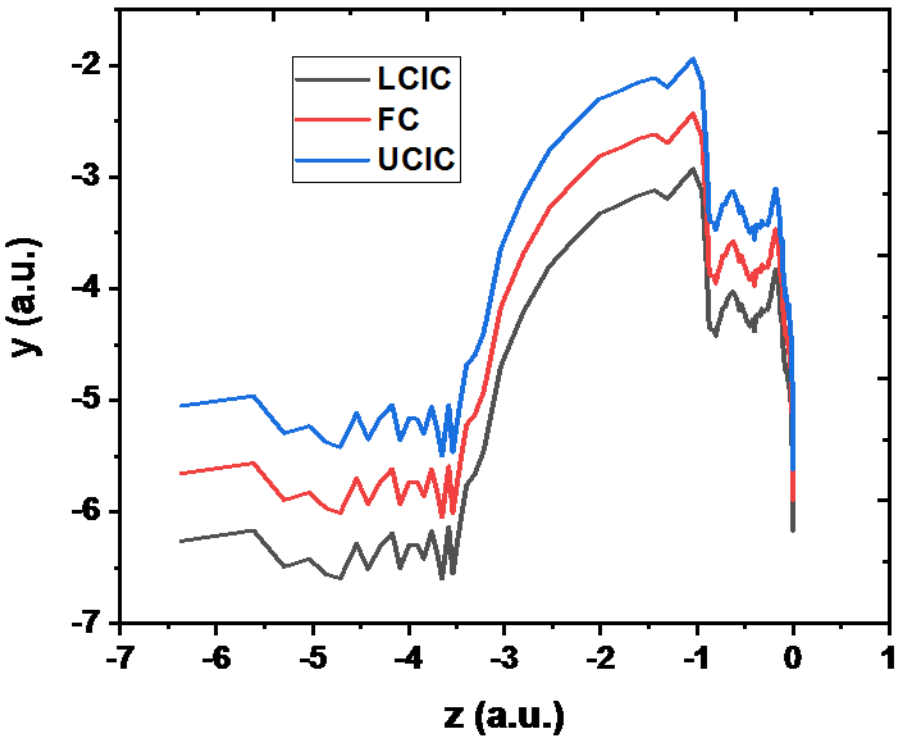

In spite of the above, as for PCO-3 hydrogel E (activation energy), A (frequency factor) and n (order of reaction) values are found to be 18.48 kJ/mol, 1.748 min-1 and 0.77 respectively. So, we have calculated values of confidence intervals (95% confidence) for each values of E, A and n, which are shown below in table:

Table 4.2- Lower confidence interval and upper confidence interval for E, A and n Value

	Lower confidence Interval	**Measured value**	**Upper confidence Interval**
E (KJ/mol)	15.43	18.48	21.53
A (min-1)	0.836	1.748	3.655
n	0.68	0.77	0.87

Among five developed hydrogel sample, we have selected one composite hydrogel sample (PCO-3) for calculating thermal degradation parameters. As our prepared composite hydrogel retains properties of biocompatibility as well as drug delivery, but alone these properties are not shown in control material (without chitosan

Oligosaccharide). Thus we calculated thermal degradation properties of composite hydrogel, but not of control material (without chitosan oligosaccharide).

4.5.3 Fourier transform infrared spectroscopy analysis

FTIR spectra of raw polymers and hydrogel composites have been shown in figure 4.5. A vibrational peak was obtained around 1096 cm^{-1} is due to the C=O stretching from remaining acetate group of PVA[199]. A peak at 1635 was obtained in FTIR spectrum of chitosan oligosaccharide due to carbonyl stretching (amide 1) of chitosan oligosaccharide. It is important to note that the composite hydrogel exhibit peak at 1640 cm^{-1} is due to C=O group. This shifting reveals the interaction between carbonyl group of chitosan oligosaccharide and hydroxyl group of polyvinyl alcohol. In all the composite hydrogel, the extent of shifting is almost same and it occurs due to the formation of hydrogen bond during the formation of composite hydrogel [200]. Appearance of peak at 1073 cm^{-1} in PCO composite hydrogels may result due to C-O stretching, indicating formation of bond between the aldehyde group of glutaraldehye with hydroxyl group of poly vinyl alcohol and chitosan oligosaccharide [201]. The prominent band exhibited by all hydrogels in the range of 3100-3600 cm^{-1} is due to the symmetric and asymmetric stretching vibrations of water molecules [202]. A peak at 1647 cm^{-1} in FTIR spectra of PCO hydrogel composite was found due to C=N stretching vibration of the imine group. This peak confirmed the crosslinking of NH_2 group of chitosan oligosaccharide and aldehyde group of glutaraldehyde [203].

The insight in the possible reaction for the crosslinking of used Poly (vinyl alcohol) and chitosan oligosaccharide can be divided into two major steps. Step 1 involves the interaction of glutaraldehyde with H^+ ions resulting into generation of carbocation. Step 2 involves nucleophilic attack on carbocation, which leads to crosslink network formation [204]. In the case of chitosan oligosaccharide, the interaction of NH_2 group

(nucleophile) of chitosan oligosaccharide with aldehyde group of glutaraldehyde leads to the formation of imine bond. Since imine bond is highly unstable, it gets converted to a C-N group[205]. Similarly, in case of PVA, it involves the reaction of OH group (nucleophile) of Poly (vinyl alcohol) with aldehyde group of glutaraldehyde, and hemiacetal bridge formation takes place [206]. The reaction scheme for hydrogel formation has been illustrated through Figure 4.6 [206, 207].

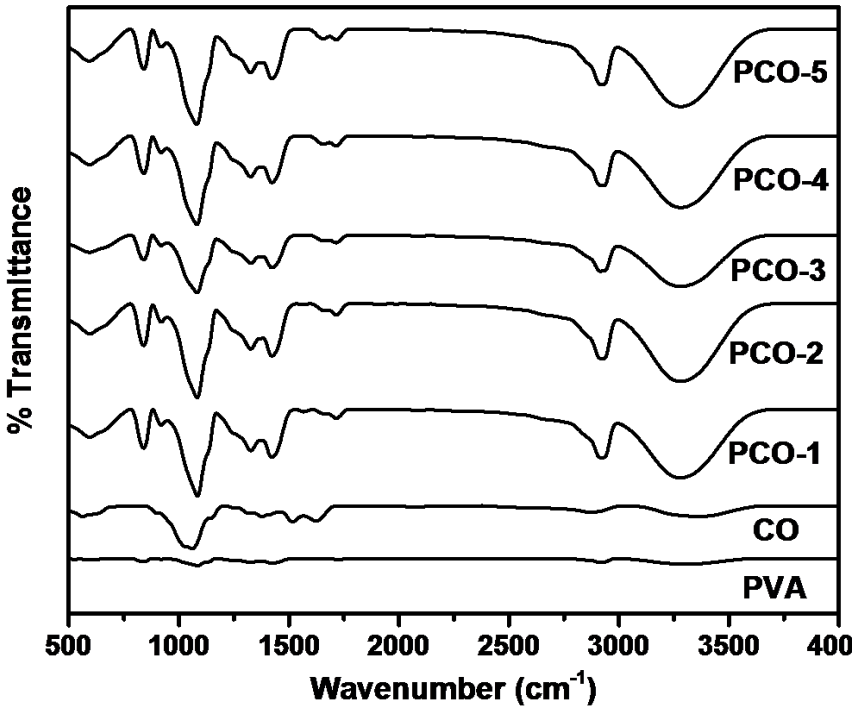

Figure 4.5: FTIR Spectra of **(A)** PVA powder, **(B)** Chitosan Oligosaccharide powder **(C)** PCO-1 Hydrogel **(D)** PCO-2 Hydrogel **(E)** PCO-3 Hydrogel **(F)** PCO-4 Hydrogel **(G)** PCO-4 Hydrogel **(H)** PCO-5 Hydrogel.

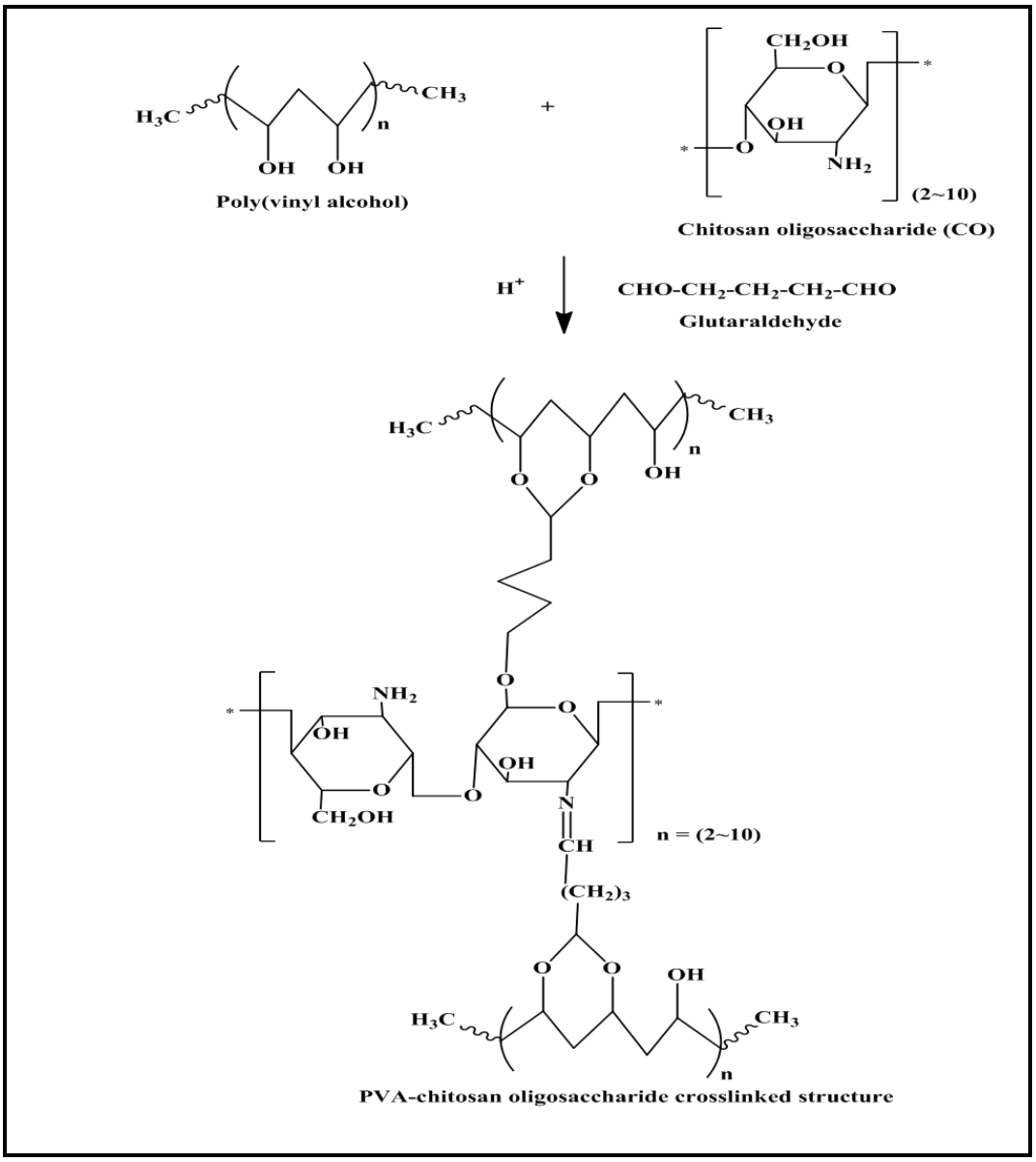

Figure 4.6: Proposed mechanism for the synthesis of PVA-Chitosan oligosaccharide composite hydrogel.

4. 5.4Stress relaxation analysis

Theσ_{max}value of PCO-1 hydrogel was observed as 0.015 Kg/ mm^2. Whereas other PCO composite hydrogel shows higher σ_{max} with respect to PCO-1 (control). This increase in σ_{max}occurs due to increase in firmness of composite hydrogel network[6]. During the stress relaxation process, all the hydrogels shows mainly two major stages, maximum stress value followed by decay in stress and achieving lowest stress value. The minimum stress value (σ_{min}) is obtained at the end of stress relaxation process. The σ_{min} value is depicts about the elastic constituent of the hydrogel. The percentage stress relaxation[6] was computed using the following equation 4.8-

$$\%\ Stress\ Relaxation = \frac{\sigma_{max} - \sigma_{min}}{\sigma_{max}} \times 100 \quad (4.8)$$

Using above equation, percentage stress relaxation of each hydrogel sample was calculated.

The percentage stress relaxation value is useful to get insight into elastic component and viscous component of the hydrogel. The 0 % stress relaxation value is exhibited by ideal elastic material, whereas 100 % stress relaxation value is exhibited by ideal viscous material[6]. The percentage stress relaxation value for the PCO composite hydrogels was found in the range of 64% to 68 %, revealing viscoelastic behavior of hydrogel composites. The percentage stress relaxation for PCO-1, PCO-2, PCO-3, PCO-4 and PCO-5 was obtained as 65%, 64%, 66%, 68% and 66% respectively. The percentage stress relaxations for PCO-2 sample is lower than PCO-1. This observation reveals that, PCO-2 hydrogel is more elastic than PCO-1 hydrogel. The remaining hydrogels composites exhibits less elastic than PCO-1 hydrogel. This result suggests that, decrease in elasticity of the hydrogel with the addition of Chitosan oligosaccharide to the composite hydrogel[6].

The model parameters[6] such as

$K_{i\to(1\ to\ 3)}(K_1, K_2\ \&\ K_3)$, K_0 *and* $\tau_{i\to(1\ to\ 3)}(\tau_1, \tau_2 \& \tau_3)$ were obtained using Weichert model (equation 4.9).

$$\sigma(t) - K_{O=} \sum_{i=1}^{n} K_{i\,exp}\left(-t/\tau_i\right) \qquad (4.9)$$

where σ(t) is attributing to the shear stress of hydrogel as the function of time t(kg/mm^2),
τ_i is attributing to the time constants of the dashpots(sec),
$n = 3$, K_i and K_o are the corresponding values for spring constant.

K_0 reveals about elastic energy in the hydrogels after completion of stress relaxation. Relaxation time is represented by τ. Instantaneous stress relaxation time (τ_1) for PCO hydrogel composite was higher with respect to Control sample (PCO-1). This result indicates that, polymer molecular arrangement process is slow upon increase in the concentration of Chitosan oligosaccharide in hydrogel composites with respect to PCO-1 sample (without CO)[6]. Except PCO-4, similar pattern in intermediate relaxation time (τ_2) was observed with PCO hydrogel composites with respect to PC0-1 sample (control). Experimental values were fitted into Weichert model and good fitting (sum of square deviation, SSD < 1) was obtained. The mechanical parameters were listed in table 4.4.

We have tested five samples. Each sample stress relaxation analyses were repeated three times. We have successfully calculated confidence Interval for percentage relaxation with 95% confidence. We have calculated lower and upper confidence intervals for percentage stress relaxation of PCO hydrogel network based on modelled (theoretical) values.

Table 4.3- Lower confidence interval and upper confidence interval for σ_{max}, σ_{min} Value for different hydrogel samples

Sample	(σ_{max}) LCI	σ_{max}	(σ_{max}) UCI	(σ_{min}) LCI	σ_{min}	(σ_{min}) UCI
PCO-1	0.0161	0.0163	0.0164	0.00542	0.00546	0.00550
PCO-2	0.0192	0.0193	0.0195	0.00591	0.00595	0.00600
PCO-3	0.0189	0.0190	0.0192	0.00584	0.00588	0.00593
PCO-4	0.0193	0.0194	0.0196	0.0056	0.0057	0.0058
PCO-5	0.0185	0.0186	0.0188	0.00571	0.00575	0.0058

Table 4.4- Lower confidence interval and upper confidence interval for % stress relaxation

Value for different hydrogel samples

Sample	(% σ) LCI	% σ	(% σ) UCI
PCO-1	66.028	66.542	67.049
PCO-2	68.784	69.257	69.723
PCO-3	68.673	69.157	69.633
PCO-4	70.133	70.631	71.120
PCO-5	68.716	69.209	69.694

Table 4.5- Mechanical Parameters of PCO Hydrogel composites

Model name	Parameter	PCO-1 (0.0019)*	PCO-2 (0.0024)*	PCO-3 (0.0021)*	PCO-4 (0.0021)*	PCO-5 (0.0022)*
Weichert model	K_1	0.107295	0.087297	0.094540	0.096646	0.087635
	K_2	0.012362	0.013041	0.013350	0.014734	0.013553
	K_3	17.332779	17.63935	18.289164	18.555765	17.664485
	τ_1	0.048620	0.336500	0.250807	0.203031	0.167546
	τ_2	10.48599	10.880456	10.997114	10.368793	10.65217
	τ_3	0.066795	0.132242	0.149641	0.149449	0.139138

K_0	0.005443	0.005932	0.005857	0.005694	0.005731
σ_{max} (kg/mm^2)	0.015	0.016	0.016	0.017	0.016
- σ_{min} (kg/mm^2)	0.005	0.0058	0.0057	0.0055	0.0056
% Stress Relaxation	65.55	64.19	66.07	68.20	66.46

*corresponds to sum of square deviation (SSD).

The K_1, K_2, K_3 and K_0 values are spring constants, and τ_1, τ_2 and τ_3 are time constants. There are no instruments available to measure these values. These values are predicted theoretically and therefore concept of precision and measurement sensitivity are out of concept here. We have calculated the confidence intervals (95% Confidence) for spring as well as time constants which are mentioned below.

Table 4.6- Maximum and minimum values of confidence interval for spring constants Value of PCO-1 hydrogel

Constants	**PCO-1**		
	Minimum CI	**Model**	**Maximum CI**
K_1	0.107295563	0.107295563	0.107295563
K_2	0.012301319	0.01236242	0.012425801
K_3	17.33277937	17.33277937	17.33277937
τ_1	0.048620137	0.048620137	0.048620137
τ_2	10.48599954	10.48599955	10.48599956
τ_3	0.066795184	0.066795184	0.066795185
K_0	0.00537433	0.00544376	0.005515781

Table 4.7- Maximum and minimum values of confidence interval for spring constants Value of PCO-2 hydrogel

Constants	PCO-2		
	Minimum CI	**Model**	**Maximum CI**
K_1	0.087296351	0.087297692	0.08729906
K_2	0.012970423	0.013041792	0.013114568
K_3	17.63935686	17.63935686	17.63935686
τ_1	0.336498816	0.336500243	0.336501698
τ_2	10.88045659	10.8804566	10.88045661
τ_3	0.132239349	0.132242662	0.132246039
K_0	0.00585137	0.00593239	0.006015007

Table 4.8- Maximum and minimum values of confidence interval for spring constants Value of PCO-3 hydrogel

Constants	PCO-3		
	Minimum CI	**Model**	**Maximum CI**
K_1	0.094540332	0.094540591	0.094540623
K_2	0.013279854	0.01335086	0.013359366
K_3	18.28916422	18.28916422	18.28916422
τ_1	0.250806647	0.25080721	0.250807277
τ_2	10.99711472	10.99711474	10.99711474
τ_3	0.149635434	0.149641735	0.149642488
K_0	0.005776473	0.005857413	0.005867109

Table 4.9- Maximum and minimum values of confidence interval for spring constants Value of PCO-4 hydrogel

	PCO-4		
Constants	**Minimum CI**	**Model**	**Maximum CI**
K_1	0.096646759	0.096646823	0.096646888
K_2	0.014653639	0.014734335	0.014817084
K_3	18.55576518	18.55576519	18.55576519
τ_1	0.203031751	0.203031972	0.203032198
τ_2	10.36879339	10.3687934	10.36879342
τ_3	0.149444179	0.149449904	0.149455771
K_0	0.005601664	0.00569474	0.005790185

Table 4.10- Maximum and minimum values of confidence interval for spring constants Value of PCO-5 hydrogel

	PCO-5		
Constants	**Minimum CI**	**Model**	**Maximum CI**
K_1	0.087635722	0.087635747	0.087635772
K_2	0.013478585	0.013553487	0.013627406
K_3	17.66448567	17.66448567	17.66448568
τ_1	0.167545935	0.167546042	0.167546149
τ_2	10.65217599	10.652176	10.65217601
τ_3	0.139132509	0.139138517	0.139144442
K_0	0.005646333	0.005731435	0.00581542

In the above mentioned data, based on the obtained 95% confidence interval, it can be stated that three digits after decimal points is justified by actual measurement.

Although these values do not appear to be significantly different, however these values have resulted from different maximum and minimum values of stress relaxation (PCO-1, PCO-2, PCO-3, PCO-4 and PCO-5).The individual values of % stress relaxation are 65.55, 64.19, 66.07, 68.20 and 66.46 for PCO-1, PCO-2, PCO-3, PCO-4 and PCO-5, respectively.

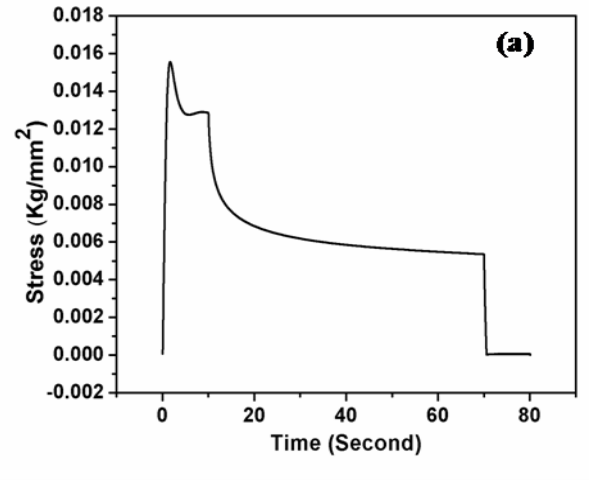

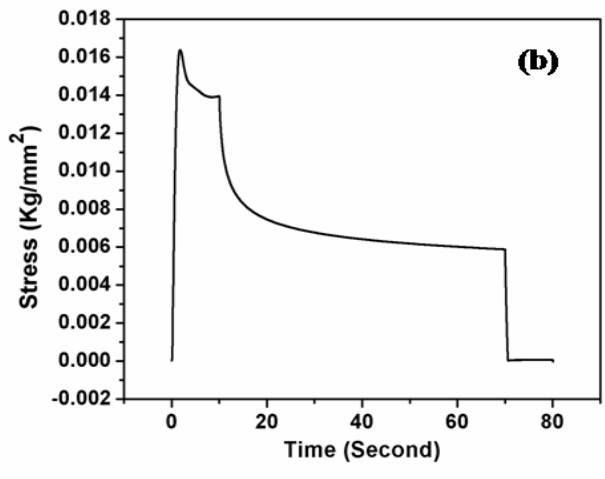

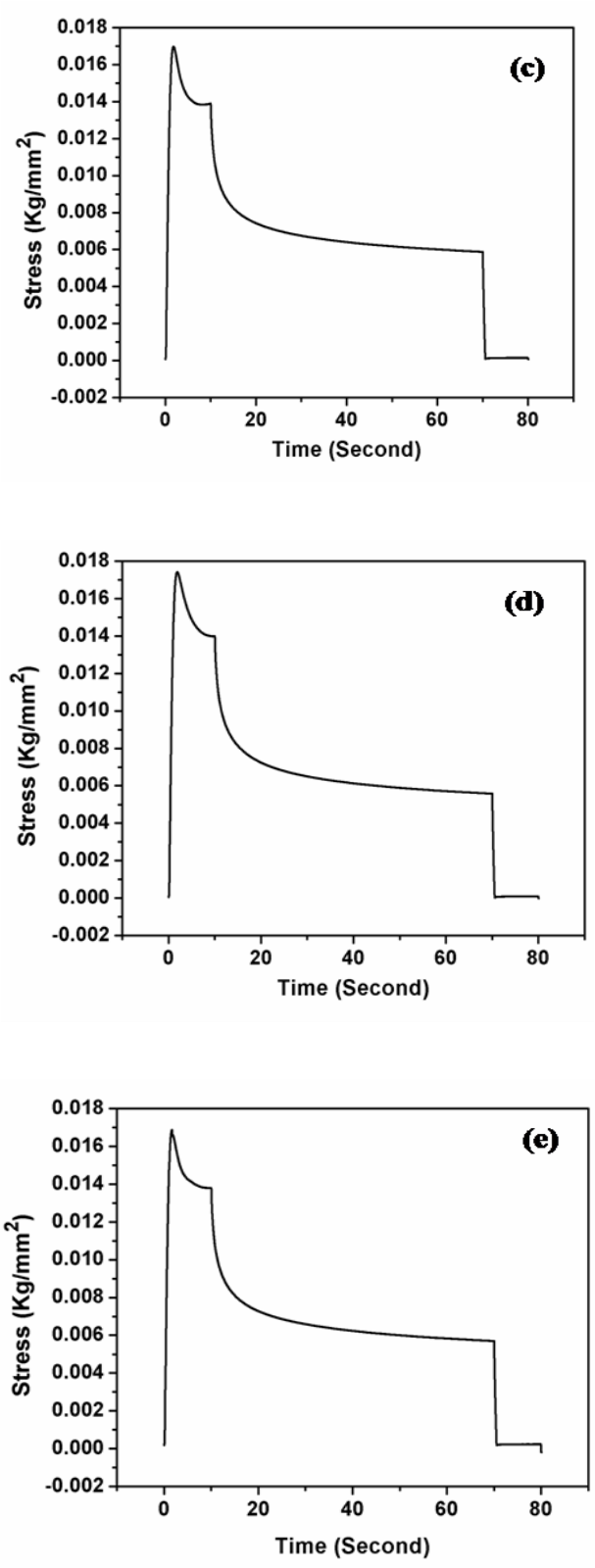

Figure 4.7: Stress relaxation study of **(a)** PCO-1 hydrogel **(b)** PCO-2 hydrogel **(c)** PCO-3 hydrogel **(d)** PCO-4 hydrogel **(e)** PCO-5 hydrogel.

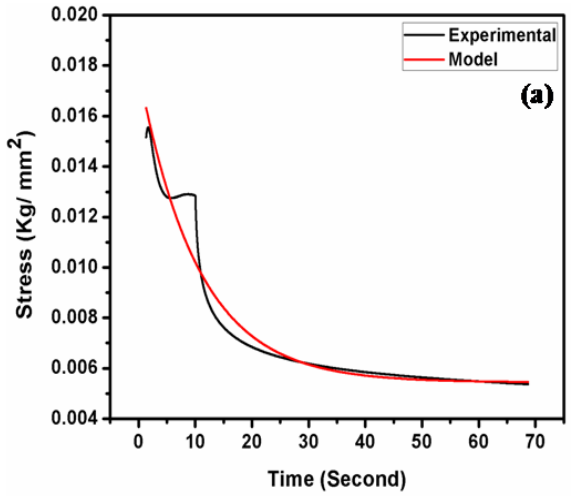
Experimental
Model
(a)
Stress (Kg/ mm2)
Time (Second)

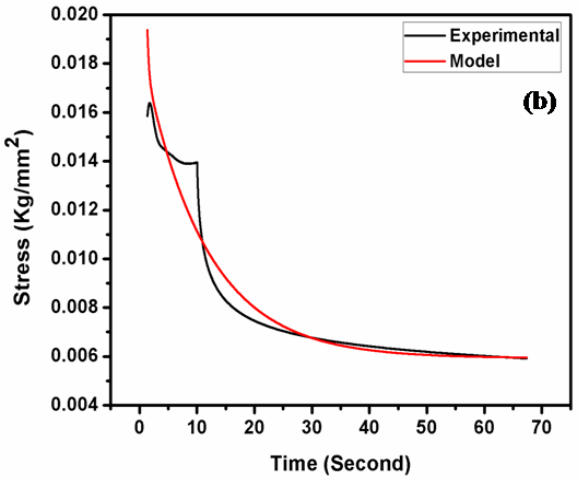
Experimental
Model
(b)
Stress (Kg/mm2)
Time (Second)

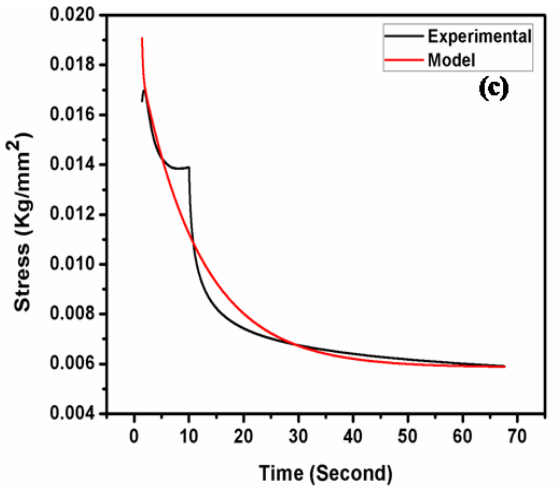
Experimental
Model
(c)
Stress (Kg/mm2)
Time (Second)

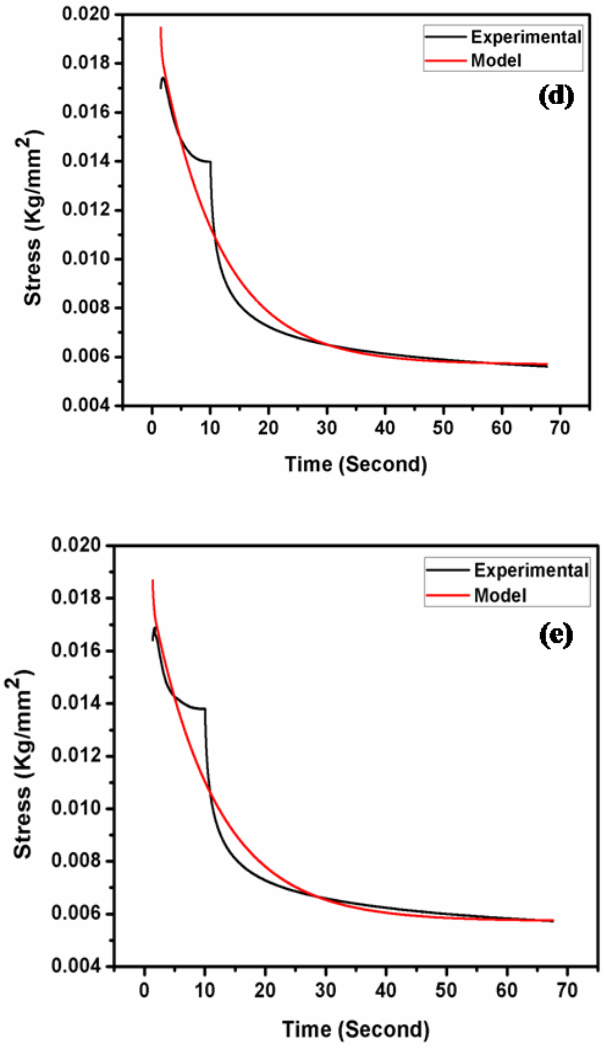

Figure 4.8: Comparison of Stress relaxation experimental result and modeling of (a) PCO-1(b) PCO-2 (c) PCO-3(d) PCO-4 (e) PCO-5 Hydrogel.

We have added curve pertaining to upper and lower values of confidence intervals and compared with the fitted curve to show accuracy of the measurement with 95% confidence.

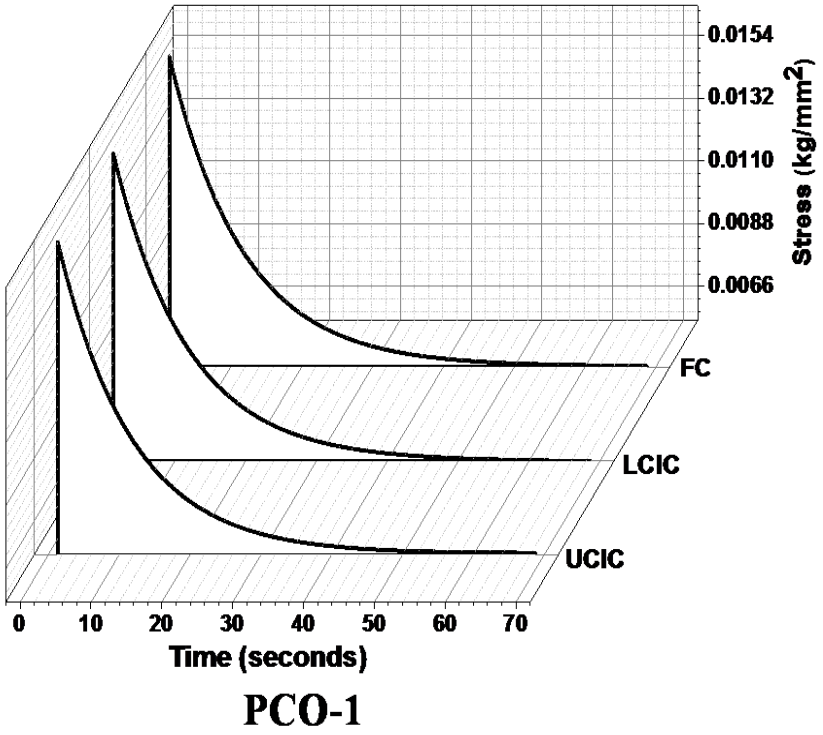

Figure 4.9 (a): Upper and lower values of confidence interval for the fitted curve of PCO-1 hydrogel.

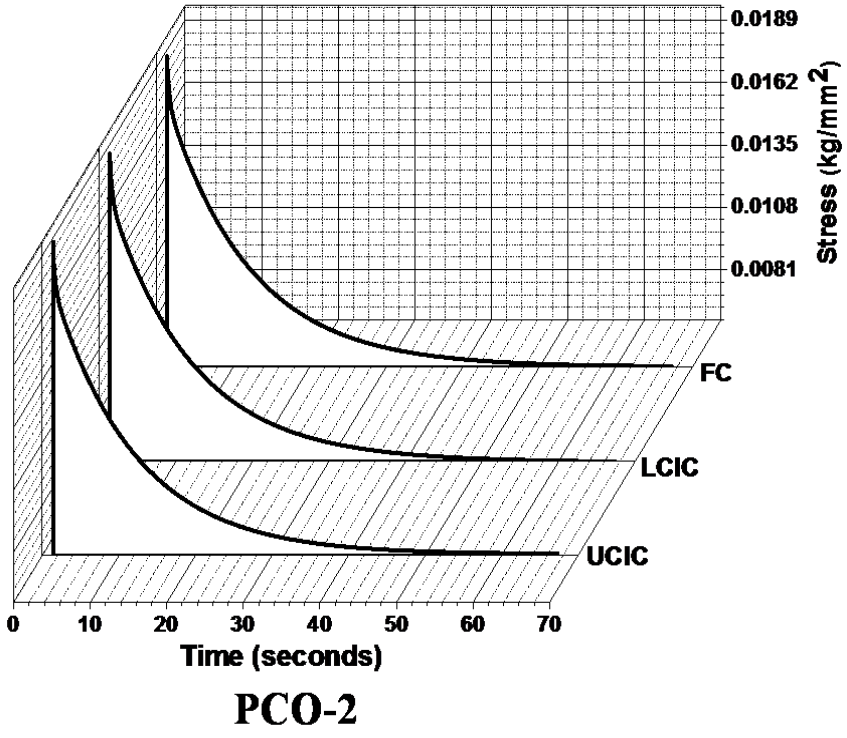

Figure 4.9 (b): Upper and lower values of confidence interval for the fitted curve of PCO-2 hydrogel.

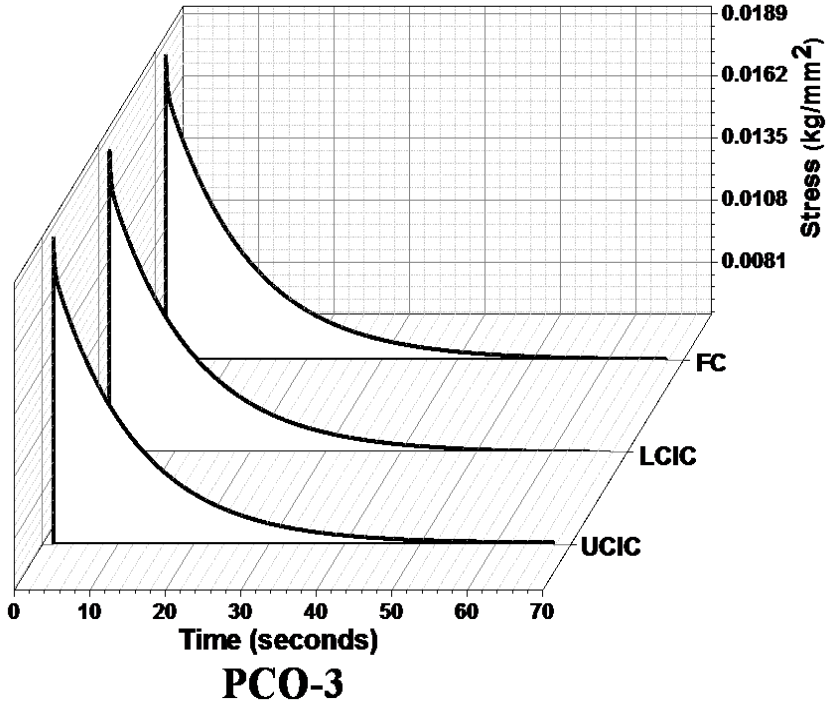

Figure 4.9 (c): Upper and lower values of confidence interval for the fitted curve of PCO-3 hydrogel.

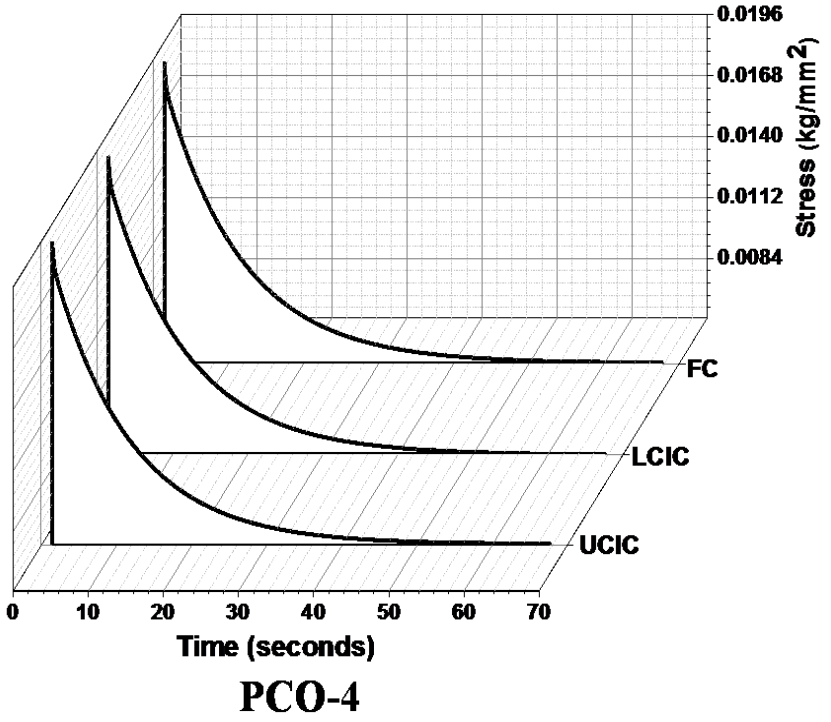

Figure 4.9 (d): Upper and lower values of confidence interval for the fitted curve of PCO-4 hydrogel.

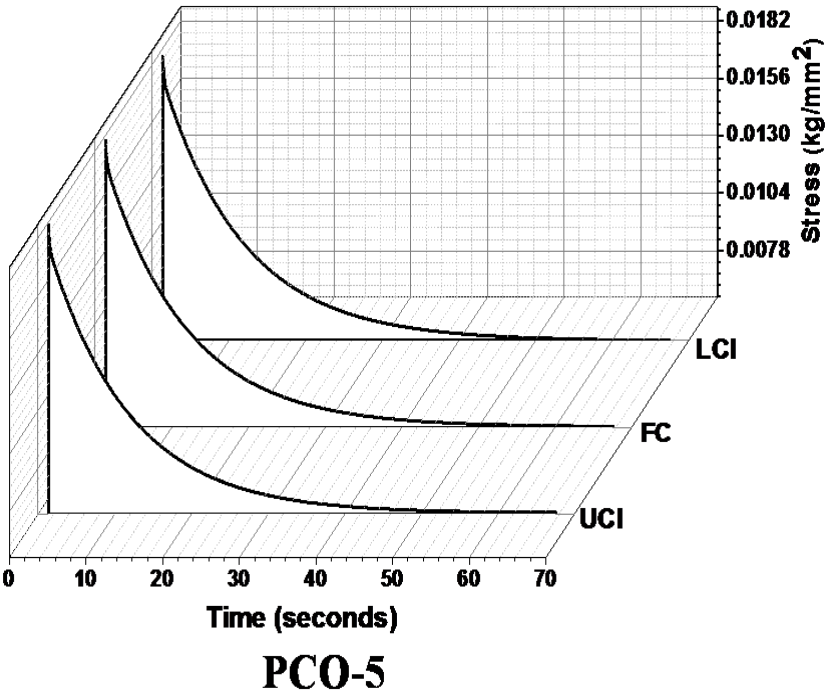

Figure 4.9 (e): Upper and lower values of confidence interval for the fitted curve of PCO-5 hydrogel.

A statistical Comparison was done by executing t-test analyses to show the differences are real or random:

For the sample PCO-1, PCO-2 and PCO-3, t-test gives p values to be 0.49, 0.45 and 0.06, respectively. Since above calculated P Values are greater than 0.05, the differences in the model and experimental mean values are random.

For the sample PCO-4 and PCO-5, t-test gives p values to be 2.01×10^{-8} and 0.0017, respectively. The calculated P Values are smaller than 0.05, and therefore the differences in the model and experimental mean values are real.

4.5.5 Surface morphology analysis

Scanning electron microscopy images (figure 4.10) of the hydrogels shows its porous nature. It has been observed that, the size of pores in hydrogels seems to be function of chitosan oligosaccharide concentration in the composite. In case of PCO-1 hydrogel (Without CO), the pore size is largest with respect to all the composite hydrogels. In contrast, PCO-5 hydrogel (highest concentration of CO) shows smallest pore on the surface of hydrogel. The decrease in pore size may occur due to increase in the number of polymeric chains in the composite hydrogels. The increase in the concentration of chitosan oligosaccharide, leads to the formation of more compact structure with smaller pores[208]. AFM studies (Figure 4.11) of all the hydrogel composite were acquired and average roughness was obtained using NOVA software. The average roughness (Ra) of PCO-1, PCO-2, PCO-3, PCO-4, PCO-5 at 10 μm was found as 0.95 nm, 3.82 nm, 6.68 nm, 0.65 nm, 5.14 nm respectively. Upon analyzing these values, it was observed that, till 1% chitosan oligosaccharide concentration increase in the surface roughness of hydrogel composite was observed. But at 1.5 % chitosan oligosaccharide concentrations, a decrease in surface roughness of hydrogel composite was observed.

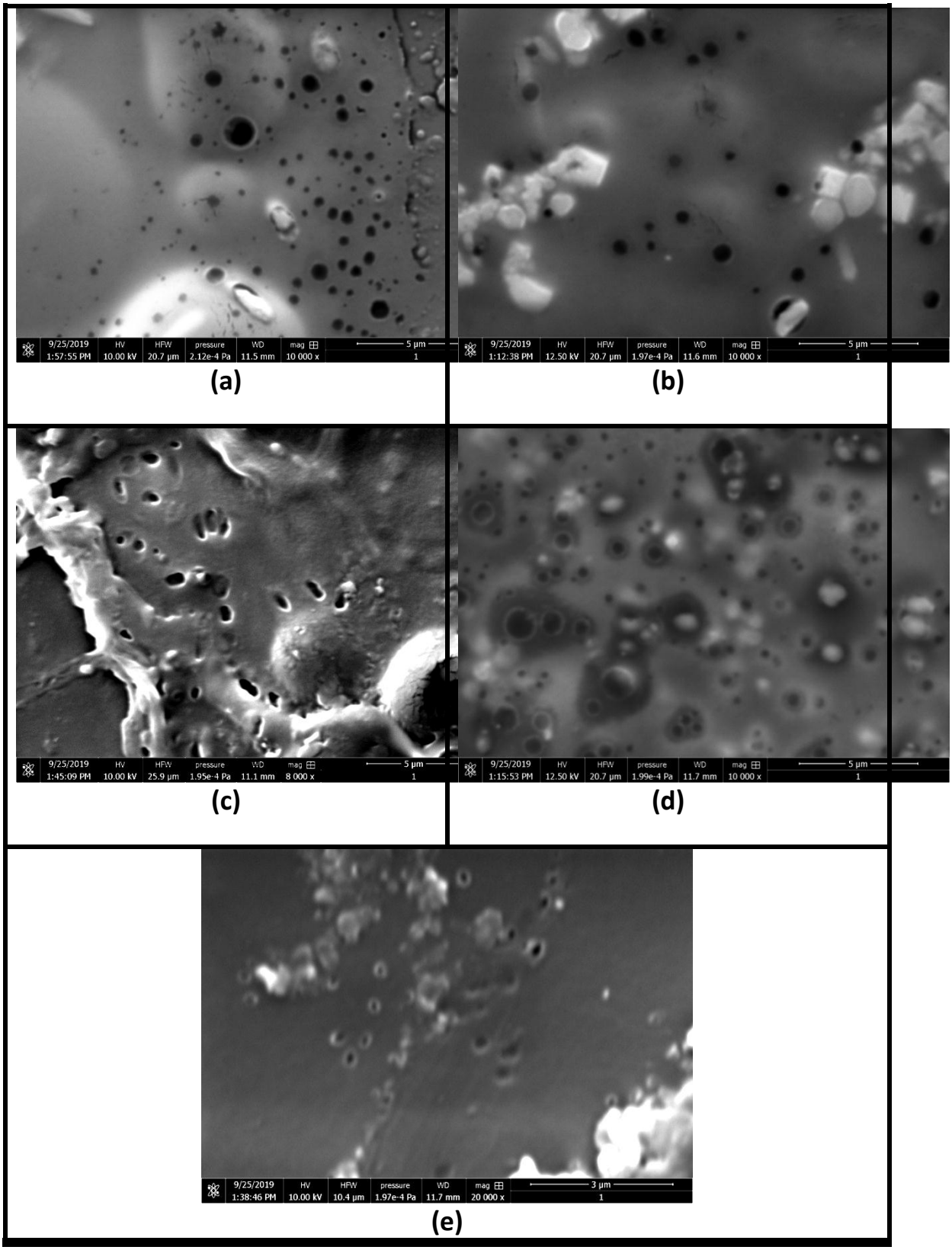
9/25/2019 1:57:55 PM HV 10.00 kV HFW 20.7 µm pressure 2.12e-4 Pa WD 11.5 mm mag 10 000 x 5 µm 1
(a)
9/25/2019 1:12:38 PM HV 12.50 kV HFW 20.7 µm pressure 1.97e-4 Pa WD 11.6 mm mag 10 000 x 5 µm 1
(b)
9/25/2019 1:45:09 PM HV 10.00 kV HFW 25.9 µm pressure 1.95e-4 Pa WD 11.1 mm mag 8 000 x 5 µm 1
(c)
9/25/2019 1:15:53 PM HV 12.50 kV HFW 20.7 µm pressure 1.99e-4 Pa WD 11.7 mm mag 10 000 x 5 µm 1
(d)
9/25/2019 1:38:46 PM HV 10.00 kV HFW 10.4 µm pressure 1.97e-4 Pa WD 11.7 mm mag 20 000 x 3 µm 1
(e)

Figure 4.10: SEM images of (a) PCO-1 Hydrogel (b) PCO-2 Hydrogel (c) PCO-3Hydrogel (d) PCO-4 Hydrogel (e) PCO-5 Hydrogel

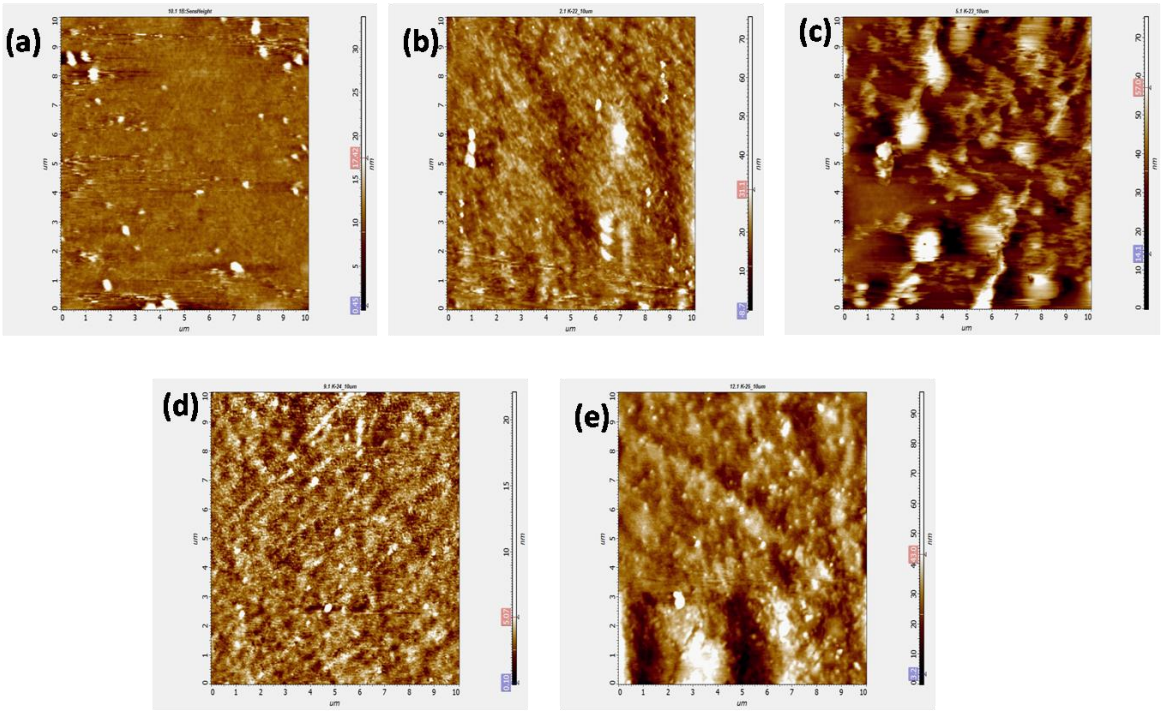

Figure 4.11: AFM image of **(a)** PCO-1 hydrogel **(b)** PCO-2 hydrogel **(c)** PCO-3 hydrogel **(d)** PCO-4 hydrogel **(e)** PCO-5 hydrogel.

4.5.6 Contact angle analysis

The contact angle (Figure 4.12) was found to be maximum (83^0) for PCO-1hydrogel sample, and minimum (63^0) for PCO-5 hydrogel sample. The surface with the contact angle ranging from 10^0 to 90^0 is considered to be hydrophilic surface. Whereas, surface with contact angle ranging from 90^0 to 150^0 is considered as hydrophobic surface[209]. The contact angle of all the hydrogels was found to be less than 90^0. The value of contact angle decreases with the increase in the concentration of chitosan oligosaccharide in the composite hydrogel**.** The protonation of $-NH_2$ group of chitosan oligosaccharide upon interaction with water results into rise in positive charge**.** Due to rise in positive charge of hydrogel composite surface, hydrophilicity of surface increases. The low contact angle

of any material is favorable for the attachment of cell over its surface[210]. Contact angle data of hydrogel unveils its, hydrophilic behavior, which increases with the addition of chitosan oligosaccharide.

The wettability of a material depends on its surface free energy. Which is governed by various factors such as chemical composition of material, and overall polarity of the material. If material possess higher surface energy than surface tension of test fluid, material exhibit low contact angle and material is considered as hydrophilic. Wettability of PCO composite hydrogel increases with increase in the concentration of chitosan oligosaccharide. It occurs due to elevation of cationic chitosan oligosaccharide concentration, which produces repulsive electrostatic forces, resulting in increase of surface free energy of the hydrogel with respect to test fluid (water). Therefore, PCO hydrogel composite having higher concentration of chitosan oligosaccharide displayed low contact angle [211].

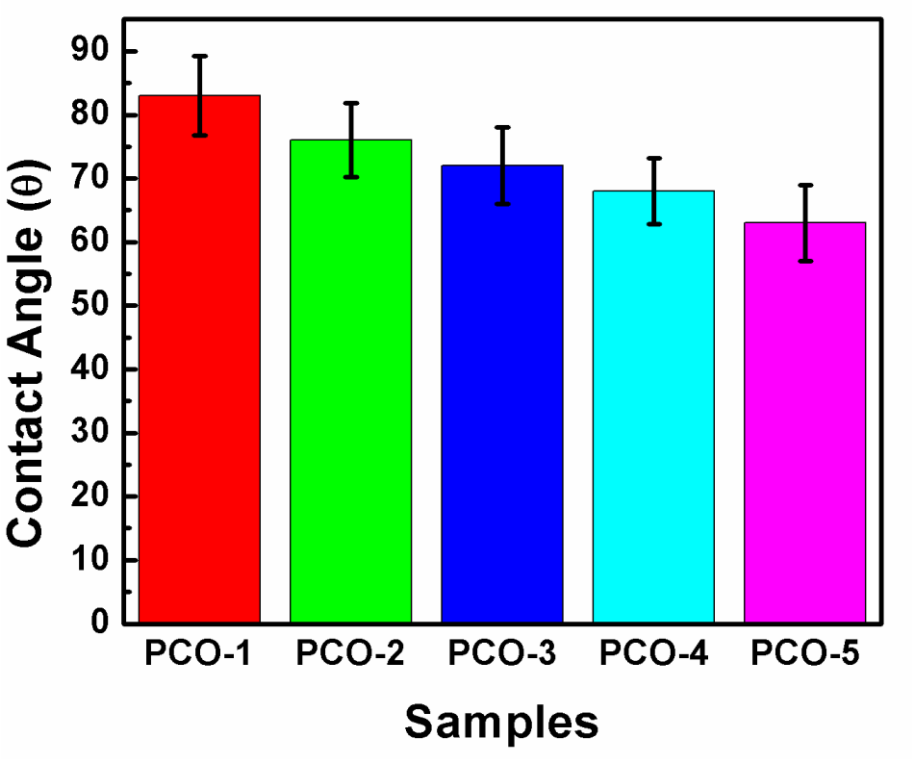

Figure 4.12: Contact Angle Study of PCO Composite Hydrogels.

4.5.7 Swelling behavior analysis

The swelling behavior of all the developed hydrogels (Figure 4.13) were performed at pH 7.4. From the swelling study data, it is clear that PCO-1 hydrogel shows lowest swelling index among all the hydrogels, whereas PCO-5 hydrogel shows highest degree of swelling. It may be due to the increase in the amount of chitosan oligosaccharide concentration in the composite, providing more number of NH_2 groups available for the formation of hydrogen bonding with water molecules. This results in the increase in swelling index[212]. The swelling behavior of polymeric network is governed by various factors such as its chemical property, solvent compatibility and extent of cross linking in the polymeric network[213]. All the hydrogels attains swelling equilibrium after almost 12 hour.

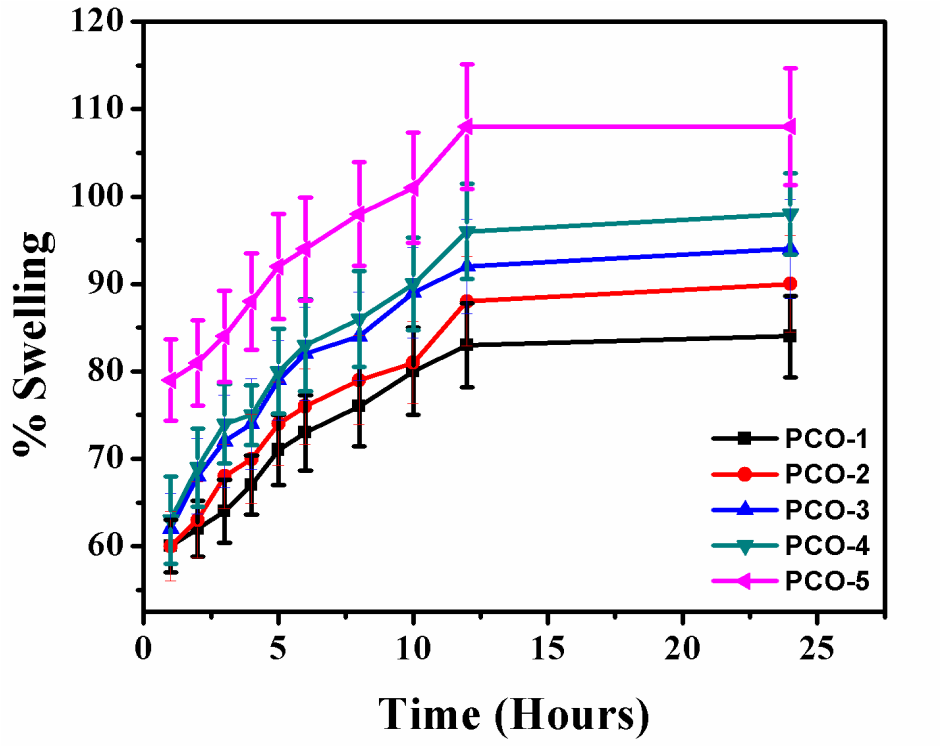

Figure 4.13: Swelling Study of PCO hydrogel Composite.

4.5.8 Drug loading, release analysis and loading efficiency

In vitro drug release study was performed for all the prepared hydrogel. The release pattern (Figure 4.14) was almost similar for all the hydrogels. Initially, all the hydrogels exhibited faster release of drugs from the hydrogel matrix. But later, all of the hydrogels displayed slower drug release. The reason for this change in release behaviorcould be due to the mobility of polymeric chains in the hydrogel network. The mobility of polymeric chain is characteristic of each polymer network.The structure of PVA and chitosan oligosaccharide has been displayed in Figure 4.1[214, 215]. Furthermore, in order to get insight into the mechanism of drug release, data were fitted into KorsmeyerPepas model[191]. The regression coefficient (R^2) after fitting with KorsmeyerPepas was found to close to 1. Therefore, no other kinetics models were considered to know mechanism of drug release[152]. After fitting the drug release data into above mentioned model, value of n was obtained. The release mechanism of hydrogel depends on the value of n. In this study, we found the n value for PCO-1, PCO-2, PCO-3, PCO-4, and PCO-5 hydrogel was 1.4, 1, 0.96, 0.82 and 0.9 respectively. Based on these n values, it can be concluded that PC0-1 and PC0-2 hydrogel follows supercase II transport mechanism, Whereas PCO-3, PCO-4 and PCO-5 follows Non- Fickian diffusion mechanism.Among these hydrogels, PCO-1 hydrogels displayed highest drug loading efficiency (Figure 4.15). Drug loading efficiency of hydrogels reduces with increase in the concentration of chitosan oligosaccharide in the composite hydrogels. It may be due to increase in compactness of the PCO composite hydrogels.

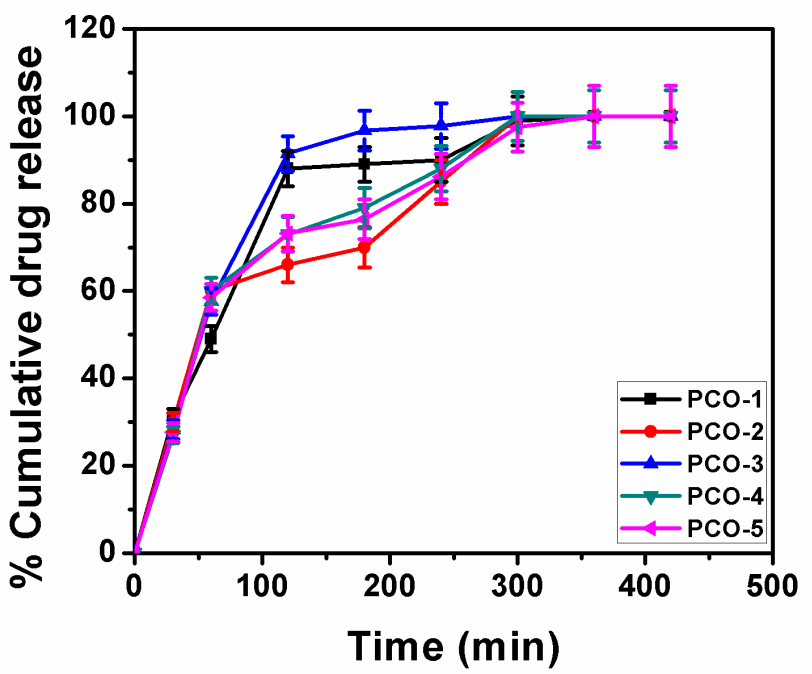

Figure 4.14: Drug release profile from PCO Composite hydrogels.

Table 4.11- Release exponent (n) of PCO Hydrogel composites

Hydrogel Sample	PCO-1	PCO-2	PCO-3	PCO-4	PCO-5
Value of n	1.4	1	0.96	0.82	0.9
Diffusion Mechanism	SupercaseII Diffusion	SupercaseII Diffusion	Non-Fickian Diffusion	Non-Fickian Diffusion	Non-Fickian Diffusion

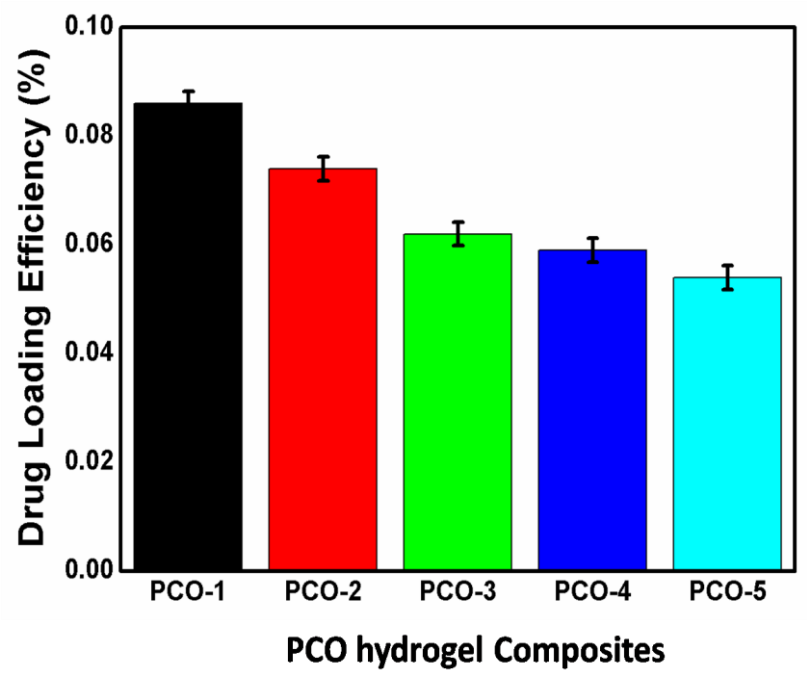

Figure 4.15: Lomefloxacin drug loading efficiency of PCO based composite hydrogels.

4.5.9 Antimicrobial evaluation

Antimicrobial study of all the developed hydrogel was estimated using disc diffusion method. The zone of inhibition formed by drug loaded hydrogel of PCO-1, PCO-2, PCO-3, PCO-4 and PCO-5 was 3.4 cm, 3.3 cm, 3.2 cm, 3.2 cm and 3.1 cm respectively (Figure 4.16). It is important to observe that, antimicrobial behavior is comprehensively exhibited by all the drug loaded hydrogel, reflecting the potency of Lomefloxacin drug to inhibit the growth of E coli bacteria. Because, Lomefloxacin is an effective antimicrobial agents used against various clinical applications, such as urinary tract infection and bronchitis[187]. Lomefloxacin, a fluorinated quinolone class antimicrobial, acts as inhibitor of bacterial topoisomerase. Fluorinated class of antimicrobial shows enhanced antimicrobial potency than non-Fluorinated antimicrobials. The antimicrobial property of Lomefloxacin (Figure 4.17) is due to presence of its 4 – Quinolone nucleus having nitrogen at position 1, ketone at position 4 and fluorine at position 7[216].

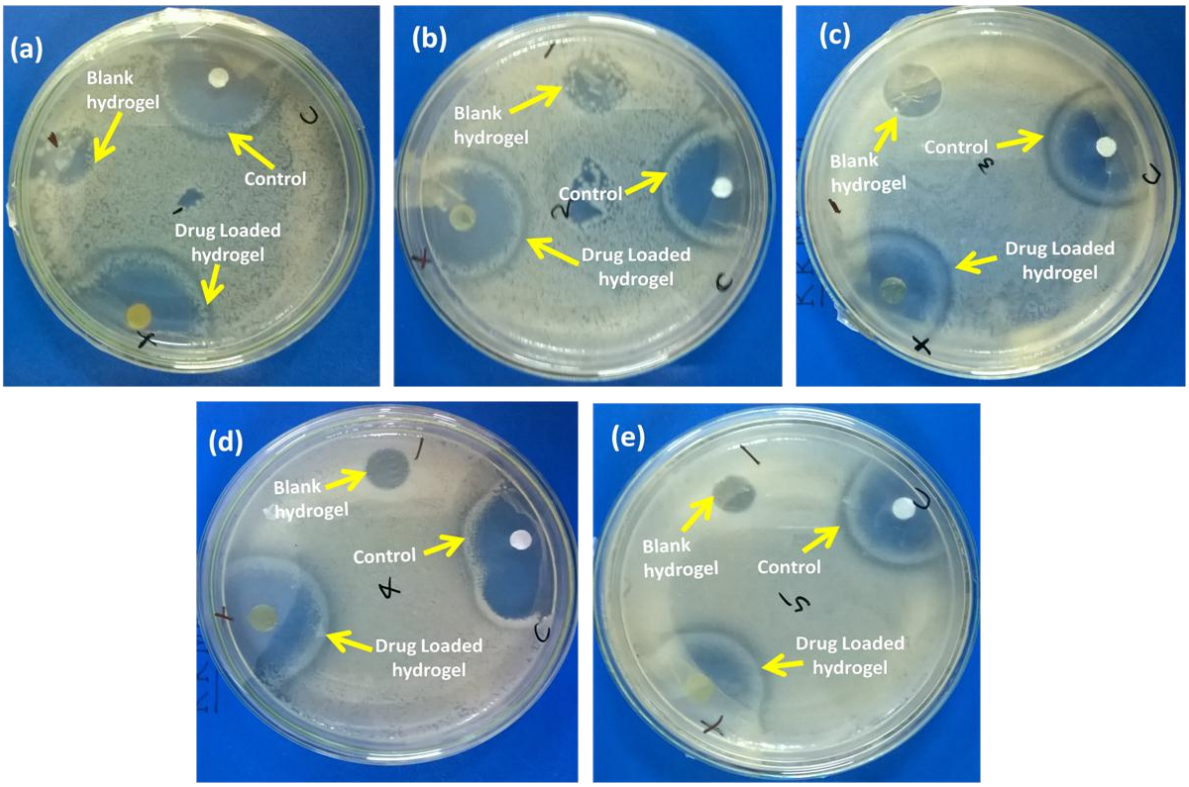

Figure 4.16: Picture showing zone of Inhibition by **(a)** PCO-1 hydrogel **(b)** PCO-2 hydrogel **(c)** PCO-3 hydrogel **(d)** PCO-4 hydrogel **(e)** PCO-5 hydrogel.

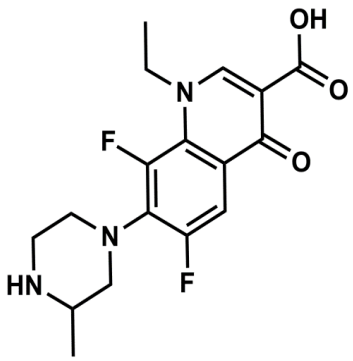

Figure 4.17: Structure of Lomefloxacin hydrochloride.

4. 5.10 In Vitro Cell Viability and Cell Imaging

In vitro cellular compatibility of hydrogels were evaluated by MTT assay. MTT assay is based upon the quantification of reduction of 3-(4, 5-dimethylthiazol-2-yl)-2, 5-diphenyltetrazolium bromide (MTT) by active mitochondrial enzymes present in the live cells[217, 218]. In the current study, higher reduction of MTT dye depicts the high survival rate of seeded cells after 24 hour, 48 hour and 72 hour. The cell viability of hydrogel composites (samples) were calculated based on the absorbance with respect to control using following formula (4.10)[155].

$$\% \, Cell \, Viability = \frac{\text{Absorbance}_{\text{sample}}}{\text{Absorbance}_{\text{control}}} \times 100 \qquad (4.10)$$

The percentage cell viability on fifth day for PCO-1, PCO-2, PCO-3, PCO-4, PCO-5 was 91%, 98%, 96%, 94% and 92% respectively. The PCO-5 shows lesser cell viability with respect to other hydrogel composites. This is due to higher compactness of PCO-5, resulting into less proliferation of cell over its surface[155]. The qualitative information about cytotoxicity of materials can be evaluated by ethidium bromide-acridine orange staining method, followed by fluorescence imaging. Live cell displays green color due to staining of its nucleus by acridine orange. Whereas, dead cells displays red color or orange color due to staining of its nucleus by ethidium bromide, upon destabilization of cell membrane[219]. The potential of PCO based composite hydrogels to support cell survival was shown (figure 10) and these hydrogels samples have shown promising cell viability and proliferation with L 929 cell line. From the MTT results, it is clear that the developed hydrogels shows magnificent growth of L 929 cell line.

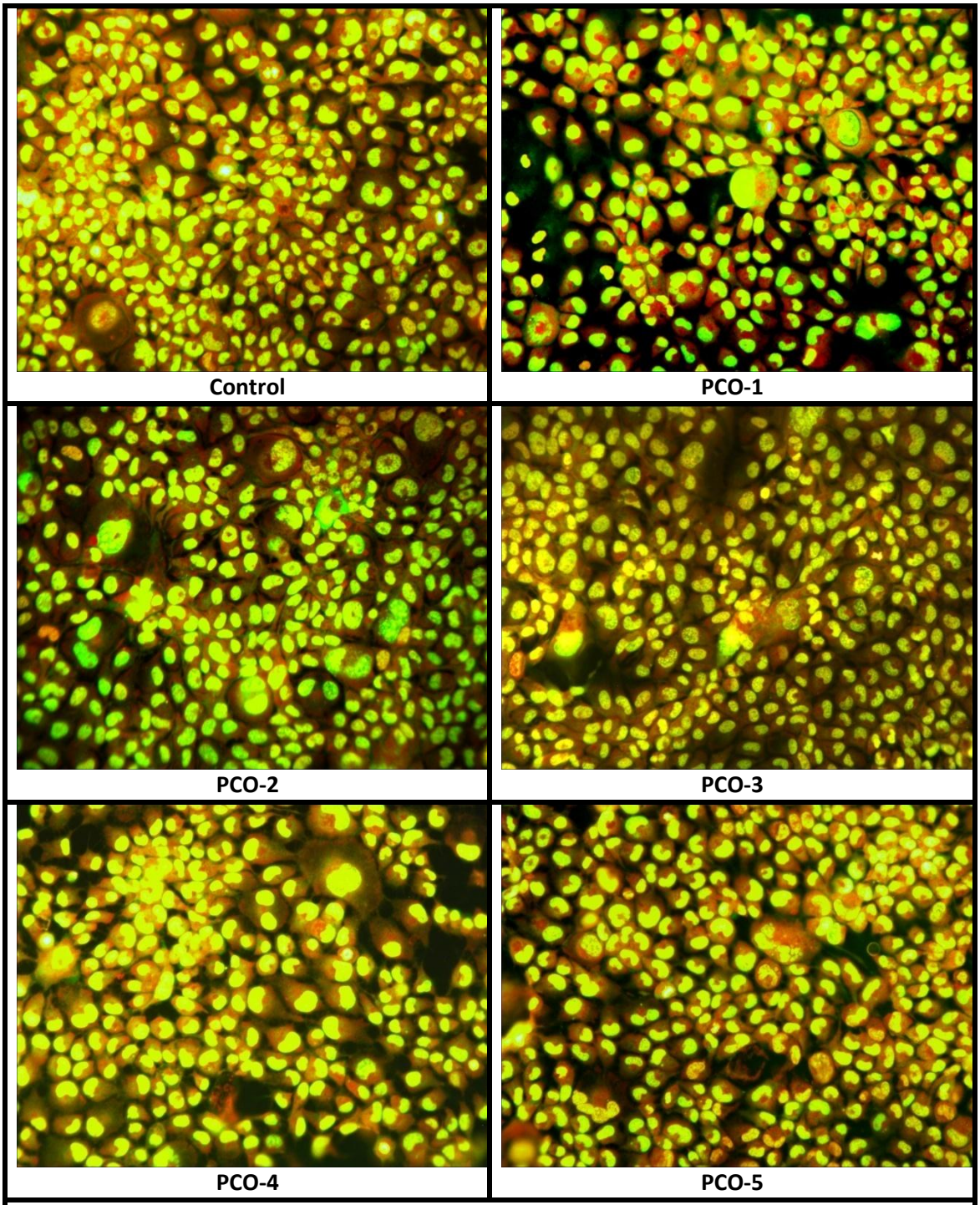

Figure 4.18(a): Fluorescence Microscopy of control and PCO composite hydrogel.

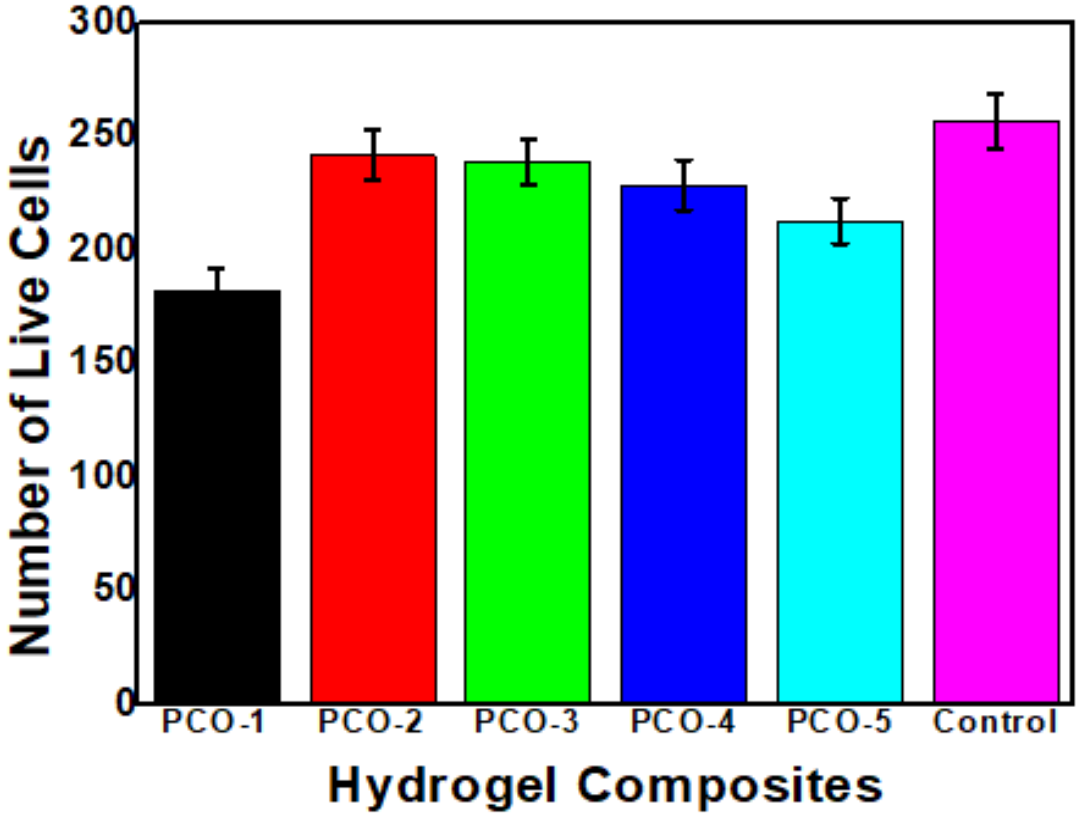

Figure 4.18 (b) Bar graph shows number of live cells present on each composite. Information was extracted using fluorescence images and Image J software.

4.5.11 Statistics studies

Statistical analysis of cell viability data was performed by t test and two ways ANOVA using Microsoft Excel Software. The difference in mean was estimated using t test. To compare between groups, unpaired student's t test was performed. Turkey's post hoc test was also used after ANOVA. This study was performed in triplicate manner. The differences in significance were presented by 'p' value < 0.05. * Which represents significant difference at the 0.05 probability level. ** represents significant difference at the 0.01 probability level. *** represents significant difference at the 0.001 level. **** represents significant difference at the 0.0001 probability level and "ns" represents non- significant difference.

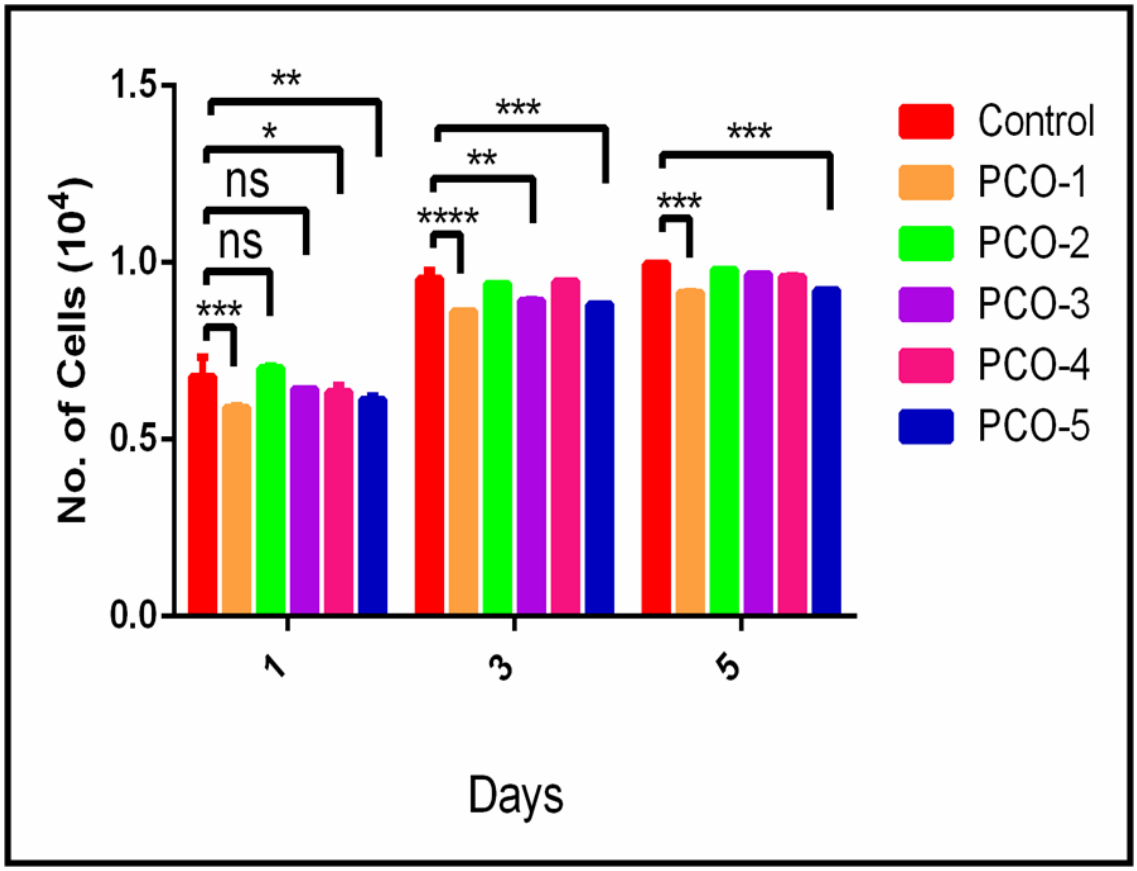

Figure 4.19- Cytotoxicity study for PCO composite Hydrogels

4.6 Conclusion

In this work, we developed a series of polyvinyl alcohol chitosan oligosaccharide composite hydrogel which were characterized by various sophisticated techniques. These hydrogel composites were developed by chemical route using glutaraldehyde as crosslinker, followed by treatment with glycine. We have shown its potential use as drug delivery matrices, using Lomefloxacin hydrochloride as model drug. This result was well supported by antimicrobial study of these drug loaded hydrogel, with effective inhibition of E. coli bacteria,due to release of drug from composite hydrogel system. The % stress relaxation increase in hydrogel composite was observed, with the increase in the concentration of chitosan oligosaccharide. Also obtained stress relaxation behavior fits well (SSD <1) with the mathematical model. Kinetic modeling was

applied to compute the thermal degradation properties of hydrogel like activation energy (18.4862 kJ/mol), frequency factor (1.74862 min^{-1}) and order of reaction (0.77). Thus, it can be concluded that, the minimum energy required to degrade the PCO-3 hydrogel was found to be 18.4862 kJ/mol. These hydrogel system exhibit high proliferation with mouse fibroblast cell line till fifth day of incubation period. Based on these outcomes, we suggest that the hydrogels would be a potential biomaterial for various bioengineering applications.